Energy Economics 155 (2026) 109200

Contents lists available at ScienceDirect

Energy Economics

journal homepage: www.elsevier.com/locate/eneco

Electric vehicles to the grid: Costs, benefits, and pricing mechanisms☆

Xuhao Zhan [a], Bowei Guo [a,b,*]

[a] School of Applied Economics, Renmin University of China, China
[b] Center for Research On Global Energy Strategy (CROGES), Renmin University of China, China

ARTICLE INFO

JEL classification:
Q41
Q55
O33

Keywords:
Cost–benefit analysis
Transportation electrification
Vehicle-to-grid
Pricing

ABSTRACT

Decarbonizing the transportation sector is essential for meeting global climate targets. However, transportation electrification imposes substantial costs on power systems. This study develops a novel data-driven approach that leverages comprehensive grid measurement data to quantify these costs, referred to here as *social costs*. The results indicate that advancements in power transfer technologies, particularly vehicle-to-grid (V2G) integration, can substantially reduce social costs and, in some cases, generate net social benefits. When the proposed method is applied to two regions in China with contrasting power system characteristics, V2G leads to significant reductions in social costs in both low (Guangdong) and high (Gansu) renewable penetration regions. The reduction is greater in Gansu, primarily driven by a stronger decline in capacity investment costs, reflecting the greater reliance of high-renewable power systems on dispatchable capacity. Based on the estimated social costs, we propose a pricing mechanism to enable economically efficient V2G integration, demonstrating the first-best market-based mechanism and the second-best direct-pricing mechanism.

1. Introduction

Decarbonization is a global imperative in the face of climate change and represents a collective effort toward achieving a sustainable future. Countries worldwide are prioritizing carbon footprint reduction to preserve ecological balance and ensure long-term economic stability, aligning with the Paris Agreement's goals. In 2022, the transportation sector accounted for approximately 24% of global carbon emissions.[1] Recognizing the sector's significant potential for emission reduction, many countries have promoted electric vehicles (EVs) to decarbonize transportation.

While electrification of transportation has significant potential to reduce carbon emissions (Shen et al., 2019), it simultaneously imposes non-negligible additional costs on the power industry. Although the fuel and carbon emission costs associated with transportation electrification are well recognized in the literature (Sovacool et al., 2017), additional expenses, such as the investments needed to improve generation capacity (Waraich et al., 2013), costs arising from transmission congestion (Green II et al., 2011; Powell et al., 2022), and expenses for ancillary services, tend to be overlooked. Collectively, these represent the social costs incurred by the power industry due to transportation electrification.

Over the past decade, power transfer technologies for EVs have evolved to mitigate the social costs associated with transportation electrification. Under conventional *unmanaged charging* (V0G), EV owners charge their vehicles based on their driving schedules, often during peak periods, thereby increasing the demand for generation capacity and adding to the social costs. In contrast, *smart charging* (V1G), which is characterized by centralized scheduling and dynamic adjustments to maintain load stability, reduces peak demand pressure and enhances grid flexibility, thereby alleviating generation capacity strain (Sovacool et al., 2017). Recently, *vehicle-to-grid integration* (V2G) has emerged as an effective solution for mitigating social costs and generating additional social benefits. By enabling EVs to discharge electricity to the grid in peak hours, V2G can reduce the demand for generation capacity and improve grid stability, offering advantages that extend beyond those of smart charging (Sioshansi and Denholm, 2010; Thompson and Perez, 2020).

This study seeks to answer three questions. (1) How do alternative charging strategies (V0G, V1G, V2G) change the social cost of electricity supply, measured in terms of fuel cost, carbon cost and generation capacity cost? (2) Do these cost effects differ across power systems with different demand profiles and renewable energy shares?

☆ Financial support from the National Natural Science Foundation of China (No. 72203218) and the Fundamental Research Funds for the Central Universities, China, and the Research Funds of Renmin University of China (No. 25XNN063) is gratefully acknowledged.

* Corresponding author at: School of Applied Economics, Renmin University of China, China.
E-mail addresses: zhanxuhao2020@ruc.edu.cn (X. Zhan), b.guo@ruc.edu.cn (B. Guo).

[1] https://www.iea.org/data-and-statistics/data-tools/greenhouse-gas-emissions-from-energy-data-explorer.

https://doi.org/10.1016/j.eneco.2026.109200
Received 24 May 2025; Received in revised form 8 February 2026; Accepted 8 February 2026
Available online 10 February 2026

(3) Which pricing mechanisms are capable of internalizing these costs and providing economically efficient incentives for V2G participation?

To answer the first question, we develop a data-driven approach to quantify the social costs imposed on the electricity industry through transportation electrification. Specifically, we evaluate how social costs vary under different power-transfer technologies, namely, unmanaged charging, smart charging, and V2G integration.

Our findings reveal a decline in the social costs as power-transfer technologies become more advanced. Unmanaged charging can result in a substantial increase in peak demand, thereby necessitating costly investments in additional generation capacity. In contrast, smart charging moderates these impacts by strategically shifting EV charging to off-peak periods, resulting in a moderate reduction in social costs. The most significant cost reduction is achieved through V2G integration. It not only alleviates peak load pressures by enabling EVs to discharge excess energy during high-demand periods, but it also incentivizes electricity price arbitrage, which further stabilizes the grid and enhances overall cost efficiency.

To address the second research question, we analyze two representative case studies of electricity systems: Guangdong province, characterized by low renewable penetration but high economic development, high electricity demand, and rich EV charging infrastructure; and Gansu province, characterized by rich renewable energy resources but low economic development, low electricity demand, and underdeveloped EV charging infrastructure. Our results demonstrate distinct social cost reduction effects of V2G across the two provinces. In Guangdong, due to high electricity demand combined with a generation mix that leans heavily on fossil fuels, V2G achieves significant social cost reductions, which mostly come from decreases in capacity investment costs related to peak-load management. In contrast, in Gansu province, due to its abundant renewable resources and high reliance on dispatchable capacity, V2G not only delivers a more substantial reduction in social costs, primarily driven by a steeper decline in capacity investment costs, but also enhances the integration of renewable energy.

To answer the third research question, we propose two pricing mechanisms to effectively internalize the social costs associated with transportation electrification. The first is a market-based mechanism that allows EV owners to participate in multiple power markets when engaging in V2G integration, such as the wholesale market and capacity market. By incorporating fuel, carbon, and capacity costs into real-time price signals, this mechanism ensures that EV charging and discharging behavior responds dynamically to the true costs of electricity generation and grid operation. Consequently, it yields the first-best outcome in terms of efficient market design.

The second is a direct-pricing mechanism that explicitly quantifies all the relevant social cost components and converts them into time-of-use tariffs for V2G integration. Compared with the market-based mechanism, this approach does not require EV owners to engage in multiple power markets, thereby significantly reducing their cognitive and learning costs. Instead, it sets time-of-use rates that reflect the estimated social costs for each hour of the day, with rates held constant across days. While this mechanism eases participation for EV users, it cannot fully capture day-to-day variations in social costs and thus constitutes the second-best solution.

Our results carry important policy implications. The findings show that both the choice of power-transfer technologies and the timing of EV charging and discharging significantly influence the social costs borne by the power sector. Unmanaged charging increases fuel consumption and capacity investment costs, whereas V2G integration substantially reduces social costs by flattening peak demand and facilitating the integration of renewable energy. The results also highlight the importance of adopting region-specific regulatory frameworks and pricing mechanisms that internalize the full social costs of transportation electrification. Particularly, the promotion of V2G technology can help alleviate grid stress by shifting peak demand to off-peak periods, while also creating additional revenue streams for EV owners through price arbitrage opportunities. Overall, our analysis offers a robust empirical foundation for policy design aimed at enhancing grid reliability and supporting a cost-effective transition to a low-carbon energy system.

The remainder of this study is organized as follows. Section 2 conducts a literature review and identifies the additional contributions of this study. Section 3 provides the institutional background and describes the current development of EVs in China as well as the electricity infrastructure in Guangdong and Gansu. Section 4 introduces the data and constructs EV charging and discharging scenarios based on different power transfer technologies. Section 5 outlines the methodology used to estimate the social costs imposed on the power sector by electrification. Section 6 presents the empirical results and quantifies the impact of transportation electrification on the power sector's social costs. Section 7 proposes market-based and direct-pricing mechanisms for EV owners under V2G integration. Finally, Section 8 concludes the study and discusses policy implications.

2. Literature review

With the increasing popularity of EVs, a growing body of research has examined the factors that affect consumer willingness to purchase EVs (Taalbi and Nielsen, 2021; Wei et al., 2021). In particular, Needell et al. (2016) found that concerns regarding the driving range considerably impede EV adoption, underscoring the pervasive impact of range anxiety on consumer behavior. Research has also explored the symbiotic relationship between infrastructure development and EV market performance. Li et al. (2017) investigated the interplay between the construction of charging stations and EV sales, revealing that subsidies for charging infrastructure are particularly effective in regions with long commuting times. McCollum et al. (2018) demonstrated that addressing non-financial consumer preferences, including improved charging infrastructure and vehicle design, is critical for promoting EV adoption in addition to fiscal incentives such as subsidies or carbon taxes. Springel (2021) found that subsidies aimed at charging infrastructure exert a stronger promotional effect on EV sales than direct purchase subsidies, whereas subsidies for charging costs are the least effective. Finally, Gillingham et al. (2023) highlighted important demographic trends and noted that urban residents, higher-income households, and people with advanced education levels are more inclined to purchase EVs.

Many studies have assessed the impact of EVs on greenhouse gas emissions. Recognizing the inherent environmental benefits of EVs, Zivin et al. (2014) examined the emission reduction potential of EVs across different power generation structures, demonstrating significant spatiotemporal variations in marginal emissions arising from differences in power plant types and operating characteristics. Their pioneering work provided an important perspective that spurred further investigation into the factors influencing EV emission reductions. Building on this, Archsmith et al. (2015) analyzed the impact of weather and temperature on battery efficiency, revealing the indirect role of climatic conditions in modulating EV emission reduction effects, offering empirical support for understanding the uncertainties surrounding environmental benefits. Subsequently, Holland et al. (2016) incorporated geographic heterogeneity and interregional pollutant transmission into their analysis. They found that, although EVs exhibit significant environmental benefits in certain regions, the overall impact is statistically insignificant. This conclusion prompted further exploration of the distributional effects of EV benefits. Building on this, Holland et al. (2019) examined the distribution of EV emission reduction effects across different income groups and societal segments, uncovering imbalances in the allocation of environmental benefits and their potential implications for policy development. More recent studies argue that earlier research likely overestimated the emissions of the internal combustion engine vehicles displaced by EVs, thereby overstating the actual emission reductions. Specifically, Davis (2019)

attributed this to EV owners driving significantly fewer miles than conventional vehicle users, while (Xing et al., 2021) found that EVs tend to replace relatively fuel-efficient gasoline vehicles, lowering the marginal emission benefits. In line with this, Muehlegger and Rapson (2023) provided further empirical evidence under different power generation structures and policy contexts and arrived at similar conclusions.

With the advancement of charging technology, an emerging strand of literature has focused on consumer participation in V2G integration. These studies primarily examined three core factors influencing consumers' willingness to engage in V2G: economic benefits, battery degradation, and flexibility requirements (van Heuveln et al., 2021; Yang et al., 2024; Suel et al., 2024; Al-obaidi and Farag, 2024; Lee et al., 2024). Regarding economic benefits, Abdelfattah et al. (2024) were the first to incorporate vehicle owners' satisfaction as a core constraint, proposing a multi-objective coordinated smart V2G integration strategy to enhance power grid performance while maximizing consumer profits. Regarding battery degradation, Wikner and Thiringer (2018) quantified the impact of different state-of-charge intervals on battery degradation, finding that avoidance of high states of charge and use of shallow cycling at low states of charge were effective in prolonging battery lifetime. Furthermore, Sagaria et al. (2025) specifically quantified the effect of V2G on the battery lifetime, revealing that calendar degradation remains the primary factor affecting battery lifetime, and the impact of V2G on battery lifetime is far lower than expected. Finally, regarding flexibility requirements, Yun et al. (2025) segmented EV consumers using a latent class conditional logit model and discussed the heterogeneous responses of different consumer groups toward V2G. Zhang et al. (2024) integrated a discrete choice experiment with latent class modeling to explore how diverse user attributes and regional characteristics influence the ultimate benefits of V2G.

Some studies focused on the impact of EV charging and discharging behaviors on power systems. Sioshansi and Denholm (2010) simulated various EV market penetration scenarios and demonstrated that V2G integration can effectively reduce power system costs while generating financial benefits for vehicle owners. Burlig et al. (2021) employed household meter data and extensive EV datasets to characterize consumer charging behavior, revealing that previous research and regulatory data may have overestimated actual EV usage. Greaker et al. (2022) used numerical simulations to explore the effects of V2G technology on consumer battery capacity choices, power load management, and overall social welfare. Their findings indicated that V2G plays a significant role in shifting peak demand to off-peak periods, thereby enhancing grid stability. Powell et al. (2022) analyzed 2.8 million charging records from 27,700 EV drivers in the United States, uncovering that EV charging behaviors could lead to the emergence of new load peaks. They emphasized that morning charging significantly promoted the absorption of renewable energy.

Recent research has increasingly focused on guiding EV-usage behavior. Ma et al. (2022) found that implementing time-of-use pricing in China effectively directs users to charge during off-peak periods, consequently lowering power supply costs. However, Bailey et al. (2024) noted that although time-of-use pricing successfully encourages off-peak charging, it also considerably increases the violations of transformer constraints during these periods, thereby incurring additional costs. Consequently, they argued that smart charging may yield more favorable outcomes. Nehiba (2024) found that EV drivers in urban areas respond more strongly to electricity price increases because they face more substitutes for private car travel and thus reduce mileage more readily. Conversely, a denser charging network increases the flexibility of charging time, allowing users to shift to lower-priced hours and thereby reducing the price elasticity of electricity demand. Consistent with this view, Bailey et al. (2023) demonstrated that EV charging exhibits high price elasticity and is significantly affected by economic incentives.

This study contributes to the existing literature in three aspects. First, although most prior research on EVs emphasized their emission reduction benefits, relatively few studies have examined the impact of transportation electrification and evolving power transfer technologies on the social costs borne by the power sector. Our proposed framework offers a comprehensive method for evaluating the economic implications of evolving power transfer technologies on power systems by separately estimating each component of the social costs.

Second, our study departs from the prevalent reliance on *ex-ante* simulation models in the EV literature by utilizing *ex-post* operational data to assess the realized impact of transportation electrification on the power sector. Specifically, we combine high-frequency generation dispatch data, marginal fuel cost and carbon price information, and system load profiles to measure the actual changes in fuel consumption, carbon emissions, and peak capacity requirements under different charging and discharging strategies. This empirical approach enables us to go beyond stylized or model-driven projections by capturing the real marginal generation units activated in response to EV charging, rather than assuming hypothetical system responses. By applying this framework to two structurally different provincial power systems, we further reveal how the social costs of EV integration vary with system characteristics, providing evidence that is both grounded in actual system operations and generalizable across regions.

Third, our work provides an integrated framework that not only quantifies the social costs and benefits of V2G integration for the power industry but also designs pricing mechanisms that effectively reflect the social costs and benefits, thereby improving market efficiency. By linking empirically grounded social cost estimates to pricing instruments, we can ensure that EV owners face price signals that reflect the true economic burden imposed on the grid. This enhances the internal consistency of our analysis and strengthens the policy relevance of our recommendations to facilitate a cost-effective transition to large-scale V2G deployment.

3. Institutional background

In 2022, approximately 10% of China's carbon emissions originated from the transportation sector, with over 80% being attributed to road transport, primarily from private vehicles (Tian et al., 2023). EVs have already made non-negligible contributions to emission reduction, and the complete transition from traditional gasoline vehicles to EVs is widely regarded as a critical step toward achieving China's climate targets (IEA, 2023). This section outlines the status of China's EV industry and its policy support. It then examines the power supply structures in Guangdong and Gansu provinces and explains their selection as case studies.

3.1. China's EV industry

The global EV market has expanded rapidly in recent years, aligned with the Paris Agreement's climate objectives. Fig. 1 illustrates annual global EV sales from 2012 to 2024. In 2024, global sales reached 17.3 million units, representing a year-on-year growth of 26%. Since 2015, China has maintained its global leadership in EV production and consumption, with 2024 sales hitting 11.3 million units, accounting for 65% of the global total.

China's EV development has been driven by strong policy support. Since the 18th National Congress of the Communist Party of China (2013), EV-related policies have become increasingly explicit and robust. Key milestones include the 2014 *Guiding Opinions on Accelerating the Promotion and Application of New Energy Vehicles* and the 2015 *Development Guide for Electric Vehicle Charging Infrastructure (2015–2020)*. In 2023, the *Opinions on Supporting the Healthy Development of New Energy Vehicle Trade and Cooperation* introduced 18 policy measures to stimulate international EV trade. These initiatives have lowered market-entry

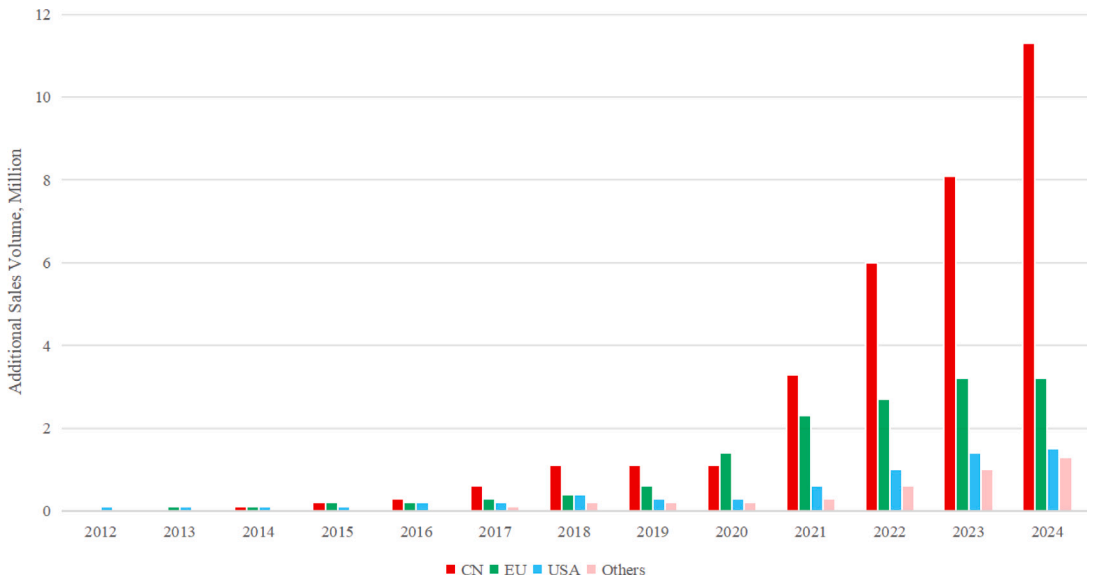

Fig. 1. Annual global new sales volume of electric vehicles, 2012–2024.
Source: The International Energy Agency (IEA).

barriers, reduced operational costs, and attracted significant private investment.

However, transportation electrification inevitably increases social costs in the power industry. To address these challenges, the 2023 *Implementation Opinions on Strengthening the Integration and Interaction between New Energy Vehicles and the Power Grid* identified V2G as a critical future development pathway.

V2G holds particular significance for China's energy transition. First, it aligns with the country's carbon neutrality goals of reducing emissions in the transportation sector by optimizing energy use and decreasing reliance on fossil fuels. Second, as EV adoption accelerates, managing the resulting surge in electricity demand has become a pressing issue. V2G can alleviate grid stress by enabling EVs to function as distributed energy storage, providing ancillary services, and enhancing resilience. Third, V2G supports innovation and economic growth, fostering new business models such as demand response programs and peer-to-peer energy trading. Its integration with smart-grid technologies has advanced energy management, contributing to China's smart city initiatives and sustainable urban energy ecosystems.

3.2. Power supply in Guangdong and Gansu provinces

To investigate how transportation electrification and emerging power transfer technologies affect power systems with different structural characteristics, this study selects Guangdong and Gansu as two representative cases.

Guangdong is characterized by a highly developed EV ecosystem and a distinctive electricity supply structure. In 2023, it ranked first nationwide in EV ownership, number of public charging piles, and number of charging stations, reflecting advanced charging infrastructure and high EV penetration driven by strong economic activity and dense urban transportation demand.[2] From the perspective of power supply, Fig. 2(a) shows that Guangdong relies primarily on conventional thermal generation and large-scale inter-provincial electricity imports,[3] while the share of local renewable energy remains relatively limited.[4] Under such a system configuration with high demand, tight supply during peak hours, and low renewable flexibility, transportation electrification tends to exacerbate peak-load stress and capacity adequacy concerns, making the deployment of V1G and V2G technologies particularly relevant. Provinces such as Zhejiang, Jiangsu, and Shanghai share the closest resemblance to Guangdong in terms of economic development level, electricity supply and demand profiles, EV penetration, and charging infrastructure maturity. Beijing, Shandong, Anhui, and Henan also exhibit similar features, though to a slightly lesser degree.

In contrast to Guangdong, Gansu represents a power system characterized by high renewable energy availability but relatively weak electrification of the transportation sector. In 2023, Gansu ranked near the bottom nationwide in EV adoption, public charging piles, and charging stations, indicating a low level of electrification and limited charging infrastructure.[5] From the electricity supply perspective, Gansu displays the opposite structure to Guangdong. As shown in Fig. 2(b), wind and solar accounted for 31% of the total power generation in Gansu in 2023. The province is a major exporter of renewable electricity to other regions; however, local demand is insufficient to absorb all available generation, resulting in persistent curtailment during low-load periods. These characteristics are broadly shared by other provinces in western China (such as Qinghai, Ningxia, Tibet,

[2] In 2023, Guangdong had 563,175 public charging piles (4.432 per 1000 people) and 27,969 charging stations (0.220 per 1000 people), far exceeding the national averages of 87,842 public piles (1.934 per 1000 people) and 5321 stations (0.117 per 1000 people) respectively. Meanwhile, the ownership of EVs in Guangdong reached 2,951,186 units (23.227 per 1000 people), which was also significantly higher than the national average of 658,420 units (14.500 per 1000 people). Zhejiang ranked second in China in terms of the number of public charging piles, with a total of 223,783 units (3.377 per 1000 people), and it also took the second place in EV ownership, recording 2,040,829 units (30.796 per 1000 people). Jiangsu, on the other hand, ranked second nationwide in the number of charging stations, with 15,028 stations in total (0.176 per 1000 people). Data: https://www.evcipa.org.cn/newsinfo/8183139.html; https://www.163.com/dy/article/J1GF3QFG05566UJN.html.

[3] In Fig. 2, the difference between aggregate power generation and total demand represents net electricity imports. A positive value indicates net imports, whereas a negative value indicates net exports.

[4] Source: wind.com.cn.

[5] Gansu had only 14,788 public charging piles (0.600 per 1000 people) in 2023, significantly below the national average of 87,842 (1.934 per 1000 people). Among comparable provinces, only Yunnan exceeded 40,000 (1.099 per 1000 people). This reflects the substantial electrification potential that remains in many western and northeastern regions.

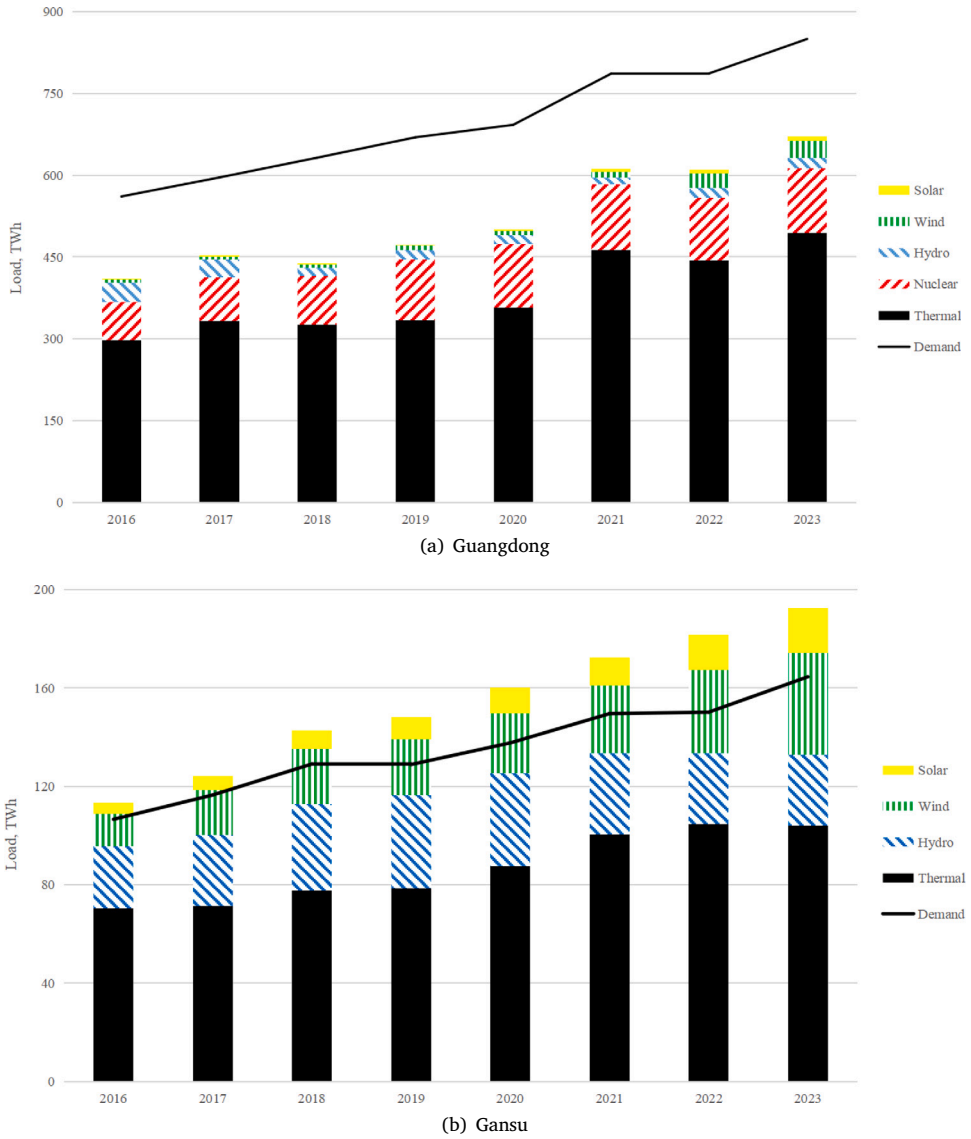

Fig. 2. Generation by fuel types and renewable penetration in Guangdong and Gansu Provinces, 2016–2023.
Source: Wind Economic Database.

and Yunnan) and northeastern China (such as Jilin and Heilongjiang). Among them, Qinghai, Tibet, and Yunnan exhibit particularly high shares of hydropower, while still facing challenges of low local demand and renewable energy curtailment. In such systems, the challenge of transportation electrification does not primarily lie in peak capacity shortages but rather in insufficient demand flexibility and effective utilization of renewable energy. V2G therefore provides value as a distributed storage resource: by enabling EVs to absorb renewable surpluses during off-peak hours and discharge when needed, it can reduce renewable energy curtailment and improve system stability.

In summary, by selecting Guangdong and Gansu as case studies, this study covers power system conditions that are representative of at least 13 provinces and two municipalities directly under the central government, accounting for approximately 52% of China's population.[6] The two provinces represent two structurally divergent yet typical system configurations in China. By covering these two contrasting extremes, the analysis spans the major spectrum of conditions under which transportation electrification interacts with the power sector in China.

Transportation electrification directly affects the electricity system by changing the load demand. Maintaining a real-time balance between the power supply and demand requires flexible supply-side adjustments. However, not all power generation facilities can accommodate such changes. Wind and solar power, with their inherent variability and unpredictability, produce outputs that are difficult to accurately forecast and dispatch. Nuclear and biomass power plants, due to their low marginal costs, are typically designated as must-run units to meet the grid's minimum stable demand, making them unsuitable for adjusting the output to match marginal load variations. Hydropower is capable of demand response but is constrained by seasonal and meteorological factors, limiting its reliability as a marginal resource. Similarly, interprovincial power transactions are often governed by medium- to long-term contracts or bilateral agreements, leaving them inflexible to short-term demand shifts. As a result, thermal power plants, particularly coal-fired units and combined-cycle gas turbines (CCGTs), are the primary facilities capable of adjusting the output to manage short-term load fluctuations and maintain supply–demand equilibrium in the electricity system. In this study, the portion of electricity demand met

[6] National Bureau of Statistics of China, https://data.stats.gov.cn/index.htm.

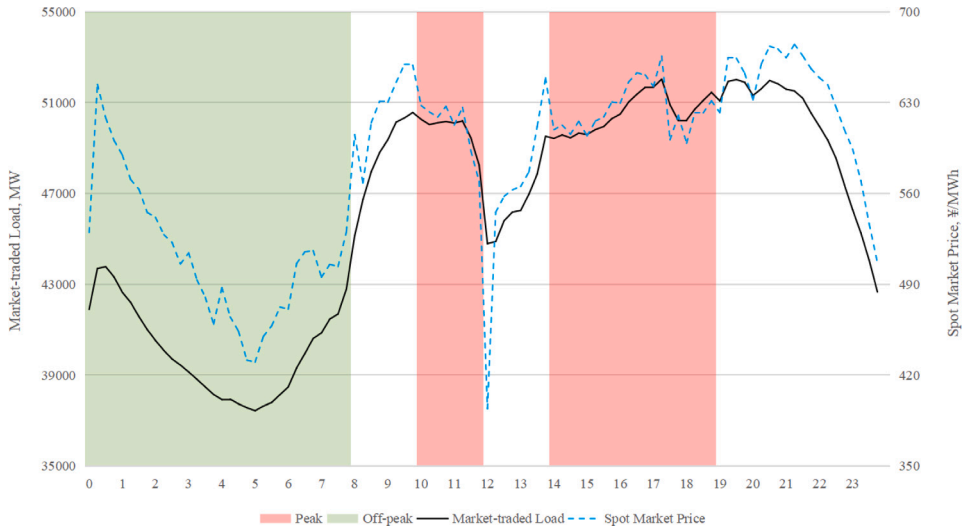

(a) Guangdong (Low Renewables)

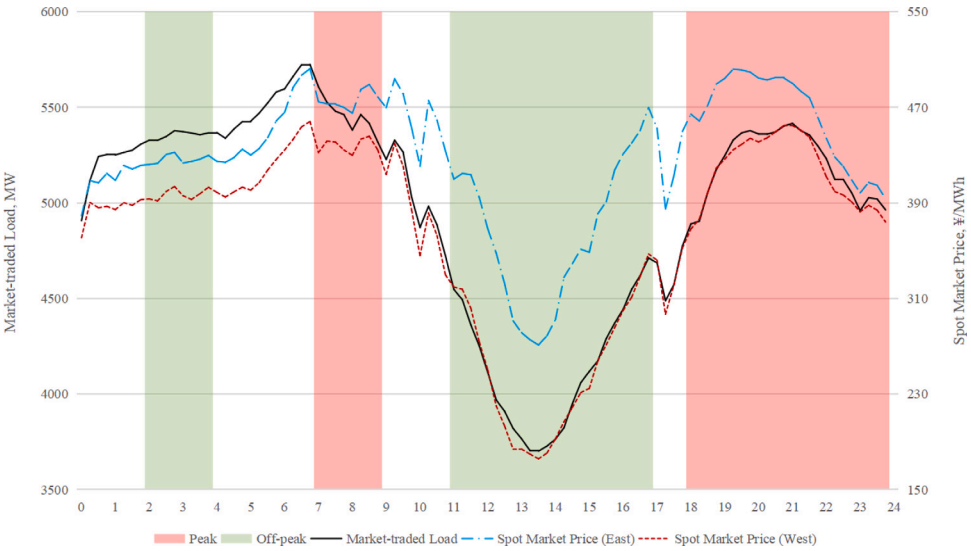

(b) Gansu (High Renewables)

Fig. 3. Market-traded load and spot market (real-time) price in Guangdong (Oct 2021–Sep 2022) and Gansu (Jan 2022–Dec 2022) Provinces.
Source: Guangdong Power Exchange Center and Gansu Power Exchange Center.[7]

by coal-fired and gas-fired units is defined as the market-traded load, as other types of generation units did not participate in the electricity spot market during the period of analysis.

Fig. 3 presents the daily average market-traded load curves and spot market (real-time) price curves for Guangdong and Gansu during the sampling period. The shaded regions represent officially designated periods for time-of-use pricing for each province. Variations in renewable energy availability, industrial structure, and economic development contributed to significant differences in the market-traded load and spot market price profiles between the two provinces.

In Guangdong, the daytime market-traded load consistently exceeded nighttime levels, with a brief reduction around midday. In contrast, Gansu experienced higher nighttime market-traded loads, with the daily minimum occurring in the afternoon owing to peak solar generation, and the market-traded load increased in the evening. Not surprisingly, the corresponding spot market prices in both provinces align closely with the market-traded load. The differences between the two provinces suggest that transportation electrification and evolving power-transfer technologies for EVs may have heterogeneous impacts on the grid.

In Guangdong, prices were highly consistent with the officially designated peak and off-peak periods. By contrast, in Gansu, the officially designated peak hours did not fully coincide with periods of high market-traded load throughout the day, and the alignment between spot market prices and the official time-of-use pricing periods was also inconsistent (see Fig. 3(b)). Consequently, if EV charging and discharging decisions are based on Gansu's official time-of-use tariff, they may not align with actual load conditions and spot market price signals, exacerbating peak-load pressures under smart-charging and V2G scenarios. The following section introduces the scenarios designed to provide detailed empirical analyses of these dynamics.

[7] During the sample period, Gansu divided the demand side into two pricing zones corresponding to the East and West regions based on grid congestion conditions. "Spot Market Price" refers to the real-time price in the corresponding zone.

Table 1
Descriptive statistics of the dataset.

Variable	Unit	Obs.	Mean	S.D.	Min.	Max.
Guangdong (Low Renewables) [Oct 2021–Sep 2022]						
Day-ahead Price	¥/MWh	35 040	562.60	190.62	0.00	1274.41
Real-time Price	¥/MWh	35 040	581.80	244.11	0.00	1500.00
Day-ahead Load	MW	35 040	82 351	24 907	27 710	145 000
Real-time Load	MW	35 040	81 273	24 364	26 154	143 330
Market-traded Load	MW	35 040	46 554	13 254	13 313	80 996
Large Coal	MW	35 040	14 541	4570	19 134	23 640
Medium Coal	MW	35 040	12 368	4057	3003	21 514
Small Coal	MW	35 040	10 909	2864	4182	17 160
Double-shaft Gas	MW	35 040	6178	2157	1999	14 729
Single-shaft Gas	MW	35 040	2557	1466	0	7058
Coal Costs	¥/ton	365	1437.39	277.09	1050.00	2600.00
LNG Costs	¥/ton	365	7306.00	1253.24	5050.00	9650.00
National ETS	¥/tCO2	365	54.77	6.37	41.46	61.38
Gansu (High Renewables) [Jan 2022–Dec 2022]						
Day-ahead Price (East)	¥/MWh	35 040	413.30	144.43	40.00	800.00
Real-time Price (East)	¥/MWh	35 040	428.10	186.72	40.00	800.00
Day-ahead Price (West)	¥/MWh	35 040	365.90	184.26	40.00	800.00
Real-time Price (West)	¥/MWh	35 040	366.30	217.98	40.00	800.00
Real-time Load (Total)	MW	35 040	20 125	2929	13 436	30 911
Market-traded Load (Total)	MW	35 040	4971	2140	0	15 361
Solar (Total)	MW	35 040	1914	2594	0	9073
Wind (Total)	MW	35 040	3920	2645	0	12 378
Coal Costs	¥/ton	365	873.60	38.93	850.00	950.00
National ETS	¥/tCO2	365	58.10	1.01	54.99	61.38

Notes: Single-shaft gas turbines are usually more efficient than double-shaft gas turbines, but less flexible. Small coal plants have a capacity of <350 MW compared with the capacity of 600–700 MW for medium-sized coal plants and >1000 MW for large coal plants.

Table 2
Characteristics of selected electric vehicles.

Vehicle model	Tesla Model Y	BYD Song Pro DM-i	BYD Yuan Plus
Category	BEV	PHEV	BEV
Battery Capacity (KWh)	60.00	18.30	49.92
Charging Power (KW)	11.00	3.30	6.60
NEDC* Range (km)	554	85	430

*NEDC: New European Driving Cycle.

4. Data and scenarios

Herein, we present a descriptive statistical analysis of the empirical data. Then, to examine the impact of transportation electrification and evolving power transfer technologies on the social costs imposed on the power industry, we develop a series of charging and discharging scenarios that simulate real-world conditions.

4.1. Data

The empirical analysis uses data from Guangdong and Gansu provinces, with slight temporal discrepancies owing to data availability. Guangdong's dataset spans one year from October 2021 to September 2022, whereas Gansu's dataset covers the full calendar year of 2022. Electricity market data, including spot market prices and load data (with Gansu's spot market divided into eastern and western parts), are obtained from the provincial Power Exchange. To identify the marginal fuel in Guangdong's electricity industry, this study incorporates 15-min real-time power generation data from various types of power plants sourced from the Guangdong Power Grid Corporation. As equivalent data for Gansu are unavailable, it is assumed that coal-fired power plants serve as the marginal fuel source, given the absence of CCGTs in the power industry.

The fuel cost estimation for thermal power plants in Guangdong relies on the price of Q5500 steaming coal at Guangzhou Port (¥/ton),[8] the delivered price of liquefied natural gas (LNG) in Guangzhou (¥/ton), and unit-specific thermal efficiency data. The efficiency data are obtained from the *Notification on the Energy Conservation and Emission Reduction of the Thermal Power Industry in Guangdong, Guangxi, and Hainan Provinces (Regions) in 2021* issued by the South China Regulatory Bureau of the National Energy Administration. For Gansu, which has no CCGTs in operation, the fuel cost is calculated solely using the price of Jingyuan Q5500 steaming coal (¥/ton).[9]

The social cost of carbon (SCC) emissions for both provinces comes from the transaction prices from the national carbon emissions trading scheme (ETS) (¥/tCO2), the reason for which is discussed in Section 5.3. China's national ETS, officially launched on July 16, 2021, postdates the sample period for both provinces.

Table 1 presents a descriptive statistical analysis of the dataset. As coal, natural gas, and ETS are traded exclusively on weekdays, missing values for weekends and holidays are linearly interpolated.

4.2. Scenario design

To comprehensively evaluate the impact of transportation electrification and evolving power transfer technologies on the social costs in the power industry, we consider three widely adopted EV models: Tesla Model Y, BYD Song Pro DM-i, and BYD Yuan Plus.[10] Table 2 summarizes the technical specifications of the selected models.[11] We also consider nine distinct (dis)charging scenarios to reflect diverse operational strategies and temporal variations. These scenarios include three distinct power transfer technologies: unmanaged charging, smart charging, and vehicle-to-grid integration, denoted as V0G, V1G, and V2G, respectively. By accounting for the unique characteristics of each vehicle model and the varying (dis)charging scenarios, our simulation framework enables a robust analysis of our research questions. Table 3 presents the detailed configurations of the nine (dis)charging scenarios analyzed in the empirical study.

[8] Q5500 refers to the coal with a net calorific value on an as-received basis of approximately 5500 kilocalories per kilogram (kcal/kg).

[9] These data are sourced from the Wind Economic Database, see wind.com.cn.

[10] Source: https://ev-volumes.com/news/ev/global-ev-sales-for-2023/.

[11] Source: https://www.bydauto.com.cn/pc/ and https://www.tesla.cn/modely.

Table 3
Scenario design for (dis)charging.

		(Dis)charging hours	
		Guangdong	Gansu
V0G	Scenario 1		+ from 08:00
	Scenario 2		+ from 14:00
	Scenario 3		+ from 19:00
V1G	Scenario 4	+ from 00:00 to 08:00	+ from 02:00 to 04:00 + from 11:00 to 17:00
V1G-O	Scenario 5	+ from 01:00 to 09:00	+ from 10:00 to 18:00
V1G-F	Scenario 6	+ from 05:00 to 06:00	+ from 13:00 to 14:00
V2G	Scenario 7	+ from 00:00 to 10:00 − from 10:00 to 12:00 + from 12:00 to 14:00 − from 14:00 to 19:00 + from 19:00 to 24:00	+ from 12:00 to 18:00 − from 18:00 to 24:00 + from 00:00 to 07:00 − from 07:00 to 09:00 + from 09:00 to 12:00
V2G-O	Scenario 8	+ from 01:00 to 09:00 − from 10:00 to 11:00 + from 11:00 to 14:00 − from 19:00 to 22:00 + from 22:00 to 01:00	+ from 12:00 to 19:00 − from 20:00 to 22:00 + from 22:00 to 01:00 − from 05:00 to 08:00 + from 09:00 to 12:00
V2G-F	Scenario 9	+ from 05:00 to 06:00 − from 17:00 to 18:00 + from 04:00 to 05:00	+ from 13:00 to 14:00 − from 06:00 to 07:00 + from 12:00 to 13:00

Notes: "+ " and "−" indicates charging and discharging, respectively. Charging ceases once the battery reaches full capacity.

EVs can be charged either at regular or fast rates. In this study, we consider both but focus primarily on regular charging as it better reflects current user behavior and avoids battery degradation concerns. Fast-charging scenarios are included only as supplementary cases to illustrate the lower-bound potential of V1G and V2G in reducing social costs.

For a consistent comparison across scenarios, it is assumed that each vehicle is charged from 0% to 100% battery state of charge (SOC). However, due to the higher degradation risk faced by batteries at low and full SOC, consumers in real-world scenarios rarely initiate charging when the battery SOC reaches 0% or charge it to 100% SOC (van Heuveln et al., 2021). Instead, they usually maintain the battery SOC within an intermediate range. Nonetheless, it should be noted that this study primarily focuses on the impact of the evolving power transfer technologies on the social costs associated with the power industry. Therefore, although this assumption may not fully reflect real-life conditions, it does not undermine the primary conclusions of this study. Despite that, one can roughly estimate the impact of a narrower charging range (e.g., from 20% to 80% SOC) by multiplying the estimated fuel costs and carbon emission costs by a corresponding ratio (e.g., 60%) and then adding the capacity investment costs.

Three V0G scenarios are designed based on the charging start times: 08:00, 14:00, and 19:00. The three scenarios correspond to users initiating the charging process upon departure for work in the morning or afternoon, or upon returning home in the evening. Charging proceeds until the battery is full.

We consider three V1G scenarios, wherein we assume that the government encourages residents to charge during periods of low electricity load, facilitated by pricing mechanisms or smart charging systems. In Scenario 4, we assume that EVs are charged during off-peak hours, as defined by official time-of-use pricing policies (recall Fig. 3). If the off-peak periods in each province are appropriately designed, it will correspond to lower social costs of charging compared to V0G. However, this scenario does not necessarily yield the lowest charging cost. This is because even during off-peak periods, significant load variations exist across hours (recall Fig. 3), resulting in different social costs of charging. However, for consumers, these hours are treated equally as they are subject to the same off-peak electricity pricing. Consequently, consumers have no incentive to specifically choose the hour with the lowest market-traded load for charging. To address this, we design an optimal V1G scenario, denoted as V1G-O (Scenario 5), which represents charging during the hours with the lowest market-traded load—thus achieving the lowest social costs of regular V1G charging. We also design a fast-charging V1G scenario, denoted as V1G-F (Scenario 6), which represents charging from 0% to 100% SOC completed within the hour with the lowest market-traded load, thus achieving the lowest potential social costs of V1G (and V0G) charging across all considered scenarios.

We consider three V2G scenarios, in which EV users aim to maximize economic gains through price arbitrage by leveraging time-of-use pricing differentials while maintaining the EV's battery level above a predetermined threshold. Specifically, we maximize consumers' gains by selecting the hours with the highest electricity prices for discharging and the lowest prices for charging. We assume that the battery level should not fall below 60% of its capacity during discharging, which can reduce battery degradation from discharging to a certain extent while increasing consumers' willingness to participate in V2G.[12],[13] Similar to the above logic, the social costs or revenues for consumers with different charging and discharging preferences can be approximated by proportionally scaling the fuel and carbon costs in our results according

[12] There is no literature specifically addressing the minimum battery capacity requirement for EV owners under V2G integration. However, existing studies typically set this threshold within a range of 10% to 60%. For example, Gomes et al. (2024) set it at 10%, Wei et al. (2021) at 20%, Sioshansi and Denholm (2010) at 30%, Peterson and Michalek (2013) at 40%, Green II et al. (2011) assumed 50%, and Guille and Gross (2009) at 60%. To maximize EV user participation in V2G integration, we choose 60% as the threshold. Consequently, our estimation of the social costs associated with V2G integration represent a lower bound of its potential impact.

[13] Geske and Schumann (2018) and Sagaria et al. (2025) argued that consumers can be roughly categorized into three groups. The first group, with high travel demands, prioritizes vehicle flexibility, is more concerned about V2G-induced battery degradation, and generally prefers to keep the EV's SOC at a consistently high level (e.g., above 80%). The second group, without frequent travel needs, focuses more on the environmental and economic value of V2G and can accept the EV's SOC falling to a relatively low level (e.g., below 20%) due to discharging. The third group falls between these two extremes: they hope to gain certain income through V2G but do not want excessively low battery levels to affect potential travel needs. This study simulates the behavior of the third group to derive a benchmark result.

to their participation ratios and then adding the corresponding capacity investment costs.

Consistent with the design logic for V1G, we develop three V2G scenarios: V2G with regular charging speeds (Scenario 7), designed based on the peak and off-peak periods defined by official time-of-use pricing policies, and optimal V2G under regular charging (Scenario 8) and V2G under fast charging (Scenario 9), designed according to actual market-traded load, denoted as V2G-O and V2G-F respectively. Fig. A.9 illustrates the SOC changes of the Tesla Model Y under V2G, V2G-O, and V2G-F scenarios in Guangdong. This study constrains a set of charging and discharging processes within a single day and assumes that both charging and discharging in V2G-F can be completed within one hour. Notably, if the time-of-use periods in each province are appropriately designed, V2G is expected to reduce social costs, and there should be no significant difference in outcomes between Scenarios 8 and 7; otherwise, it may lead to an increase (rather than a reduction) in social costs.

Finally, to simplify the analysis, we assume a 90% efficiency for both charging and discharging processes, consistent with relative literature.[14]

5. Methodology

Transportation electrification increases the load demand, resulting in increased social costs in the power industry. These costs include fuel costs, carbon emissions, and investments in power plant capacity required to maintain the supply–demand equilibrium.

In this section, we introduce a data-driven approach for quantifying the impact of transportation electrification on the social costs. This approach comprises three steps: identifying the marginal power generation units, estimating each component of the social costs, and aggregating them. The second step is the foundation for designing efficient pricing mechanisms for V2G integration in Section 7.

5.1. Marginal power generation units

In a perfectly competitive electricity market, the dispatch of power generation units is expected to follow the merit-order principle. This principle dictates that power plants are dispatched in the ascending order of their marginal generation costs, which helps formulate a virtual electricity supply curve known as the merit-order curve (Chyong et al., 2020). However, physical constraints, market power, and other factors often cause the actual power-supply curve to deviate from the merit-order curve. When power dispatch data are unavailable, the merit-order curve serves as an effective proxy for the market supply curve; when such data are accessible, marginal units can be estimated through empirical modeling. Due to differences in power generation structure and data availability between Gansu and Guangdong, we apply different but robust methodologies to identify their marginal power generation units.

5.1.1. Methodology for Gansu: Merit-order Proxy

Due to the absence of publicly available power dispatch data in Gansu province, this study employs the merit-order curve as the market supply curve to identify Gansu's marginal power generation units given the load demand, as presented in Fig. A.10. During the sample period, thermal power generation in Gansu was primarily provided by 20 coal-fired power units owned by 10 enterprises, among which 17 units had an installed capacity of over 650 MW. This relatively homogeneous generation structure makes the marginal cost of each unit both observable and stable over time, as it is primarily determined by coal prices and heat rates. Unlike in provinces with a diverse mix of coal and gas plants, the dispatch order in Gansu is largely consistent with marginal cost ranking. As a result, the merit-order curve provides a reasonable and reliable approximation of the actual supply curve for identifying marginal units.[15]

5.1.2. Methodology for Guangdong: Regression analysis

Unlike Gansu, high-frequency power dispatch data are accessible in Guangdong province, enabling the estimation of marginal units using *ex post* regression analysis. Drawing on the methodologies of Cullen (2013), Novan (2015), and Guo et al. (2023), this study employs the following specification to determine the marginal power generation units across different periods in Guangdong province:

$$G_{f,d,h,t} = \alpha_{f,h,0} + \alpha_{f,h,1} R_{d,h,t} + \theta_{f,h} X_{d,h,t} + \epsilon_{f,h,t}, \quad \forall f, h \tag{1}$$

where f is the type of power plant, d is the day, h is the hour within a day, and t is the quarter-hour interval. $G_{f,d,h,t}$ is the power generation of plant f at quarter t of hour h on day d. $R_{d,h,t}$ is the corresponding market-traded load, $X_{d,h,t}$ includes the time fixed effects, and $\epsilon_{f,h,t}$ is the residual term.

As we apply Eq. (1) to each type of power plant every hour of the day, the coefficient $\alpha_{f,h,1}$ represents the frequency at which power plant f serves as the marginal unit during hour h. As Eq. (1) estimates the conditional correlation between $G_{f,d,h,t}$ and $R_{d,h,t}$ instead of their causal relationships, we directly apply the ordinary least squares (OLS) method to estimate $\alpha_{f,h,1}$. Fig. A.11 presents the composition of marginal power plants estimated based on actual power dispatch data in Guangdong.

5.2. Electricity generation fuel cost

Marginal power plants respond to marginal changes in load demand, affecting the fuel cost of generation, which depends on the fuel prices and thermal efficiency of the different types of power plants. Therefore, the impact of a change in load demand on fuel costs can be estimated using the following formula:

$$S_g = \sum_d \sum_h \sum_t \left(\sum_f \hat{\alpha}_{f,h,1} C_{f,d} \right) \cdot \left(q'_{d,h,t} - q_{d,h,t} \right) \tag{2}$$

where S_g is the impact of transportation electrification on fuel costs. In Guangdong, $\hat{\alpha}_{f,h,1}$ are the estimates from Eq. (1), indicating the frequency with which different types of power plants respond to load changes in a specific period. $C_{f,d}$ is the marginal fuel cost of power plant f on day d, calculated based on fuel prices and the corresponding thermal efficiency.[16] Thus, $\sum_f \hat{\alpha}_{f,h,1} C_{f,d}$ represents the marginal fuel cost of power generation during a specific period. $q_{d,h,t}$ is the actual load

[14] Wu and Lin (2021) assumed both charging and discharging efficiencies to be 86.6%; Nagel et al. (2024) set the charging efficiency at 93% and the discharging efficiency at 90%; Lee et al. (2024) adopted a uniform value of 96% for both charging and discharging efficiencies. Additionally, Zhang et al. (2024) showed the impact of temperature on the charging and discharging efficiency of EVs, revealing that the efficiency approaches 100% during spring and autumn in Japan.

[15] World Resources Institute released a global power plant dataset covering 35,000 units across 167 countries from 2018 to 2021, which includes geographic coordinates, capacities, plant names, and ownership information for 24 coal-fired units in Gansu province, China. In 2016, Gansu issued the *Comprehensive Plan for Ultra-Low Emission and Energy-Saving Retrofit of Coal-Fired Power Plants* (the "Retrofit Plan" hereafter), mandating low-carbon retrofits for eligible operational coal-fired plants by setting specific energy-saving targets and project deadlines, as well as an average coal consumption target for the province's coal-fired units. The Retrofit Plan provided detailed information on 20 operational coal-fired plants in Gansu in 2016. By cross-referencing these two datasets, we obtain 2022 coal consumption data points for these 20 plants (totaling 18,080 MW, accounting for 87% of the capacity). For the remaining four units not covered by the Retrofit Plan, we assume that their coal consumption aligns with the average provincial target.

[16] Table A.2 presents basic information regarding different power plants in Guangdong in 2021.

demand in the specific period, while $q'_{d,h,t}$ is the counterfactual load demand in different charging and discharging scenarios (discussed in Section 4.2). $\left(q'_{d,h,t} - q_{d,h,t}\right)$ is the difference in electricity load between the actual and counterfactual scenarios. Eq. (2) illustrates that the change in fuel cost is equivalent to the product of the load difference and the marginal cost of electricity generation.

Notably, in Gansu, where marginal units are identified using the merit-order curve rather than regression analysis, the marginal generation at any given time is supplied by a single class of coal-fired units rather than a mix of different technologies. This assumption also applies to the subsequent calculations of the social costs of carbon emissions.

5.3. Social cost of carbon emissions

Transportation electrification can also influence carbon emissions owing to changes in load demand. This impact is also dependent on the marginal plants at different periods. In general, the carbon intensity of CCGTs is lower than that of coal plants, and large coal plants emit less carbon than smaller plants because of their higher thermal efficiencies. Consequently, the periods in which the CCGTs and large coal plants act as marginal units tend to have lower marginal emissions. The economic impact of the load changes on carbon emissions is estimated using the following formula:

$$S_c = p_d^c \cdot \left[\sum_d \sum_h \sum_t \left(\sum_f \hat{\alpha}_{f,h,1} E_f\right) \cdot \left(q'_{d,h,t} - q_{d,h,t}\right)\right] \tag{3}$$

where S_c is the economic impact of transportation electrification on carbon emissions, p_d^c is the social cost of carbon (SCC), and E_f is the marginal emissions of the power plant f. Therefore, the term $\left[\sum_d \sum_h \sum_t \left(\sum_f \hat{\alpha}_{f,h,1} E_f\right)\left(q'_{d,h,t} - q_{d,h,t}\right)\right]$ represents the effect of transportation electrification on power generation carbon emissions.

Notably, p_d^c captures the economic value of carbon emissions, which varies by country. The specific value of the SCC depends on factors such as the national economy, discount rate, and extent of global warming impact. Although China has not published official SCC figures, Ricke et al. (2018) estimated China's SCC across four dimensions—social economy, climate, damage, and discount. They found that within a 66% confidence interval, the SCC per ton of carbon dioxide ranged between $4 (≈¥28) and $50(≈¥350). Our study adopts the daily average national ETS prices of China as a proxy for China's SCC. Notably, the mean value of SCC in China for the year 2021 was ¥46.3 and for 2022 was ¥58.1, both of which fell within the confidence interval recommended by Ricke et al. (2018).

5.4. Generation capacity investment cost

Generation capacity investment cost refers to the additional investment required to construct power plants to meet the growth in electricity load demand. This expansion is necessitated by the potential increase in peak load owing to transportation electrification. Notably, because V2G integration can reduce the peak load, the promotion of such technology is anticipated to reduce the need for capacity installation, thereby lowering the associated costs.

In the restructured electricity markets of some Western countries, where pricing mechanisms that reflect the reliability of thermal power generation units are well established, their capacity value can be reflected through capacity market trading prices or capacity compensation mechanisms (Callaway et al., 2018). However, given that China has not yet established a capacity market and its capacity compensation mechanism is still immature,[17] this study refers to Callaway et al. (2018) and employs the following formula to estimate the impact of electrification in the transportation sector on capacity investment costs:

$$S_k = \frac{1}{\text{count}(d)}\left(\max_{h,t}\left\{\sum_d q'_{d,h,t}\right\} - \max_{h,t}\left\{\sum_d q_{d,h,t}\right\}\right) \times K \tag{4}$$

where, S_k is the impact of transportation electrification on the capacity investment cost and $\text{count}(d) = 365$ is the total number of days within the sample period. Therefore, $\frac{1}{\text{count}(d)} \max_{h,t}\left\{\sum_d q_{d,h,t}\right\}$ and its counterpart $\frac{1}{\text{count}(d)} \max_{h,t}\left\{\sum_d q'_{d,h,t}\right\}$ are the maximum average daily market-traded load in the actual and counterfactual scenarios, respectively. Finally, K is the effective capacity construction, operation, and maintenance costs of the newly constructed capacity to satisfy the increased load demand.

In Eq. (4), the value of K is key to estimating the generation capacity investment cost. Our study refers to the *Projected Costs of Generating Electricity, 2020 Edition* published by the International Energy Agency (IEA) and the OECD Nuclear Energy Agency (NEA) (NEA, 2020) to ascertain the value of K. The report details the levelized cost of electricity generation (LCOE) of 243 types of power plants in 24 countries, including 475 MW CCGTs and 347 MW coal plants in China. The LCOE estimates the construction, operation, maintenance, fuel, and carbon emission costs per MWh for different plant types. To avoid double counting, K includes only the construction, operation, and maintenance costs within the LCOE.

5.5. Social cost

Transportation electrification affects the power system through multiple cost channels. In the main context, we focus on three core components of social costs, namely fuel costs, carbon emission costs, and capacity investment costs. For completeness, system operation costs, in particular transmission congestion costs (S_t) and ancillary services costs (S_a), are evaluated separately in Appendix A.1.

Due to data availability constraints, these operational cost components are empirically estimated only for Guangdong, where nodal prices allow us to approximate transmission congestion costs and the coexistence of real-time and day-ahead spot markets enables a tractable estimation of ancillary services costs. Even so, we acknowledge that the underlying datasets are not sufficiently granular to recover exact system dynamics. Accordingly, we adopt a pragmatic approach that combines observed market outcomes with the help of machine learning methods to approximate congestion patterns and ancillary service costs under alternative charging scenarios, offering a replicable template for data-limited settings.

Collectively, these costs are denoted as social costs S and can be estimated using the following formula:

$$S = S_g + S_c + S_k + S_t + S_a \tag{5}$$

For example, to estimate the social costs imposed on the power industry by transportation electrification under Scenario 1 in Table 3, we first assume that a specific EV model (i.e., Tesla Model Y, BYD Song Pro DM-i, or BYD Yuan Plus) initiates charging at 08:00 with a fully depleted battery (0% state-of-charge) and continues until it is fully charged. Based on the technical specifications provided in Table 2, we estimate the vehicle's impact on the electricity load and

[17] In 2020, preliminary attempts at capacity compensation were initiated in provinces, such as Guangdong, Shandong, and Shanghai . These attempts included charging capacity compensation fees based on the difference between actual and contracted electricity usage, implementing capacity compensation electricity prices, and establishing a capacity market. However, a unified system has not yet been formed. It was not until 2023 (post the sample period), when the National Development and Reform Commission and the National Energy Administration issued the *Notice on Establishing a Mechanism for Coal-Fired Power Pricing*, that China's coal-fired power sector transitioned from a single electricity price to a two-part electricity pricing system. This reform formally established a nationwide capacity pricing mechanism, reflecting the value of capacity.

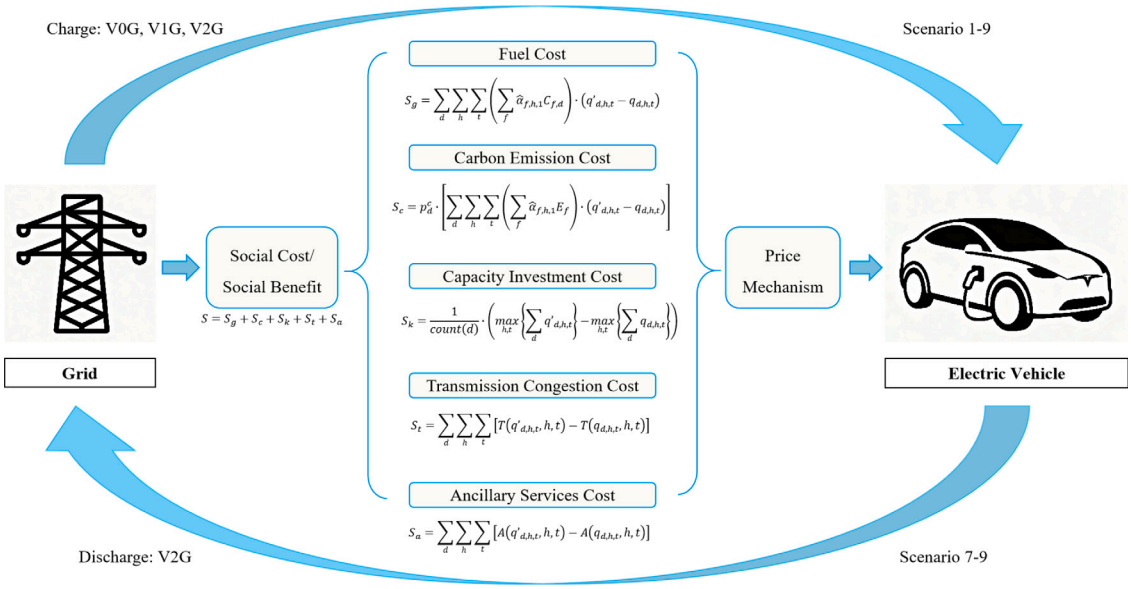

Fig. 4. Framework for analyzing the impact of transportation electrification on the social costs.

then assess how these load changes affect the social costs within the power industry. Finally, to determine the marginal impact per 100 km driven, the estimated social costs are divided by the full-charge driving range of each vehicle, calculated by dividing battery capacity by power consumption per 100 km.

Finally, Fig. 4 illustrates the overall research framework of this study. Transportation electrification influences the power system by altering electricity demand on the grid side, which subsequently generates various components of social costs, including fuel costs, carbon emission costs, and capacity investment costs, as well as transmission congestion and ancillary services costs. These system-level impacts are then transmitted back to EV users through appropriate price mechanisms, forming a closed feedback loop between the electricity system and the transportation sector. This framework links EV charging and discharging behaviors with their corresponding social costs and provides the basis for the quantitative estimation conducted in the following analysis.

6. Results

This section employs the data-driven approach introduced in Section 5 to estimate the impacts of transportation electrification and evolving power transfer technologies on the social costs in the power industry, taking Guangdong and Gansu provinces as case studies. We further translate these social costs into driving costs per 100 km to facilitate a comparison with conventional gasoline vehicles.

6.1. Social cost in Guangdong (low renewables)

As noted earlier, the social costs of transportation electrification consist of fuel costs, carbon emission costs, capacity investment costs, as well as system operation costs such as transmission congestion costs and ancillary services costs. The latter two components are calculated separately in Appendix A.1. Our estimates show that, under current market conditions in Guangdong, the combined contribution of transmission congestion and ancillary services costs accounts for only a very small proportion of total social costs (see Table A.1). Therefore, the main text focuses on the three dominant cost components when presenting and interpreting the results (namely, fuel, carbon, and capacity investment costs). Nevertheless, this does not preclude the possibility that, with higher levels of EV penetration, deeper V2G participation, and increasing variability from renewable integration, the operational costs of congestion management and ancillary services may become more significant in the future.

Fig. 5 illustrates the impact of transportation electrification on the social costs in Guangdong's power industry under nine scenarios, based on a dataset spanning October 2021 to September 2022. The detailed values for each scenario are presented in Table A.3.

There are notable differences in the social costs across the three unmanaged charging scenarios (Scenarios 1–3). Scenario 2 incurs the highest social costs owing to peak-hour charging, which intensifies the demand for additional generation capacity. In this scenario, fuel costs and capacity investments account for 60% and 37% of the social costs, respectively, whereas carbon emissions contribute <3%. In contrast, Scenarios 1 and 3, in which charging does not impact the maximum load demand, do not require additional capacity investment. In these cases, fuel costs dominate, accounting for approximately 95% of the social costs.

Smart charging (Scenarios 4–6) substantially reduces social costs compared with Scenario 2, in which unmanaged charging intensifies peak load stress and increases capacity investment needs. However, when compared with Scenarios 1 and 3, the reduction in social costs is relatively modest. This difference highlights that the primary value of smart charging lies in avoiding charging during peak-load hours, thereby mitigating the need for additional generation capacity required to accommodate transportation electrification. By contrast, the shift from unmanaged to smart charging has only a limited impact on fuel and carbon emission costs. This is mainly because the composition of marginal generation units in Guangdong remains relatively stable throughout the day, resulting in minimal variation in marginal fuel consumption and carbon emissions across hours.

Furthermore, the comparison among Scenarios 4–6 shows that although both V1G-O (Scenario 5) and V1G-F (Scenario 6) achieve additional reductions in social costs relative to regular V1G (Scenario 4), the gains are very limited. This indicates that Guangdong's existing time-of-use tariff design is already effective in encouraging users to avoid charging during peak-load hours, thereby capturing most of the capacity-saving potential. As a result, further refinements in charging timing or charging speed generate only marginal additional benefits.

Scenario 7, which represents V2G operation under regular charging speeds, highlights the substantial potential of EVs to relieve peak-load stress and lower overall system costs. Although the additional charging–discharging cycles lead to higher energy losses, the ability of EVs to discharge electricity during peak hours significantly reduces the

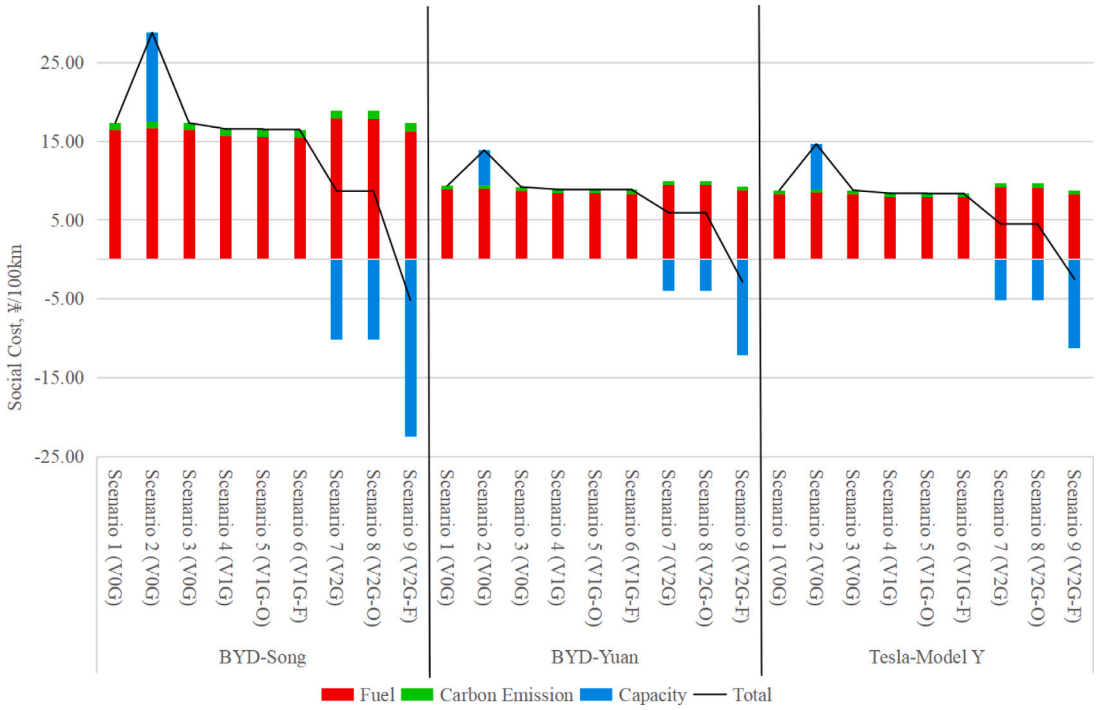

Fig. 5. Social costs of transportation electrification in Guangdong Province (Oct 2021–Sept 2022).
Notes: The horizontal axis categorizes the three selected EV models under nine distinct (dis)charging scenarios—comprising three unmanaged charging (V0G) scenarios, three smart charging (V1G) scenarios, and three V2G scenarios. The vertical axis measures the social costs in ¥ per 100 km, whereas the different colored bars represent the various cost components that collectively form the social costs. The black curve shows the trend in social costs as the power transfer technologies evolve from V0G to V1G to V2G.

need for additional generation capacity, resulting in a net decrease in social costs.

V2G-O (Scenario 8) further lowers social costs compared with Scenario 7 and yields the optimal outcome under regular charging conditions. However, similar to the comparison between V1G and V1G-O, the additional reduction is limited, as most of the capacity-saving benefits have already been captured under Scenario 7. In contrast, V2G-F (Scenario 9) produces a more pronounced reduction in both fuel costs and capacity investment costs. The decline in fuel costs arises from strategically charging during the lowest-cost hours and discharging during the highest-cost hours, thereby maximizing the price differential between charging and discharging. Meanwhile, the reduction in capacity investment is driven by the higher discharge power during peak-load hours, which more effectively offsets system peak demand and diminishes the need for new generation capacity.

Fig. 5 also shows the variations in social costs across different vehicle types. BEVs such as the BYD Yuan and Tesla Model Y exhibit similar impacts on the power industry, whereas the PHEV BYD Song incurs higher costs owing to its lower energy-conversion efficiency. Notably, the driving cost per 100 km for the Tesla Model Y under unmanaged charging (up to ¥14.7) is markedly lower than that of a conventional gasoline vehicle, as exemplified by the BMW 3 Series (¥70.3). This highlights the substantial economic and social benefits of electrification.[18]

[18] The calculation of social costs for gasoline vehicles primarily includes the costs of fuel and carbon emissions. Fuel costs are derived from the retail price of national 95-octane gasoline in 2022 (data source: Wind Database) and the fuel consumption rate of the BMW 3 Series per 100 km. Carbon emission costs are calculated based on the average carbon emissions per 100 km for gasoline-powered vehicles in China and the transaction price of national carbon emission allowances in 2022.

6.2. Social cost in Gansu (high renewables)

Fig. 6 illustrates the impact of transportation electrification on social costs in Gansu's power industry, using a dataset covering the entire year 2022, with details presented in Table A.4.

In Gansu, Scenarios 1, 3, 4, 5, and 6 resemble their counterparts in Guangdong. Social costs are primarily driven by fuel costs (approximately 88%), with carbon emissions accounting for 12%. However, there are significant cost differences between the two provinces. For example, the social costs of traveling 100 km in Scenario 1 with a BYD Yuan is ¥9.3 in Guangdong but only ¥3.8 in Gansu. This disparity is due to differences in power generation structures: in Gansu, the marginal load is only met by coal plants, whereas in Guangdong, it is shared by both coal plants and CCGTs. Because CCGTs have substantially higher generation costs than coal plants, and coal prices are much lower in Gansu than in Guangdong during the sample period (see Table 1), EV fuel costs are significantly lower in Gansu, leading to lower social costs.

Scenarios 2 and 7 in Gansu differ substantially from those in Guangdong. In Gansu, the generation capacity investment cost remains negligible across three unmanaged charging scenarios. This is primarily because the province's market-traded load peaked at approximately 6:00 (see Fig. 3(b))—a period not allocated for charging or discharging in Scenarios 1–7. This phenomenon has become increasingly common in regions with a high share of renewable energy, where the load curve exhibits a "duck curve" pattern. Examples include Shandong province in China and California in the United States. Notably, under Scenario 7 (V2G integration with regular charging speeds), EV charging and discharging adhere to the officially defined peak and off-peak periods. However, the designated peak period fails to capture the actual peak in the market-traded load, resulting in the limited impact of V2G integration in reducing social costs. In contrast, under Scenario 8 (V2G-O), EVs determine charging and discharging based on the actual fluctuations in market-traded load. As in Scenario 8 for Guangdong, the load-aligned strategy substantially lowers generation capacity investment costs and,

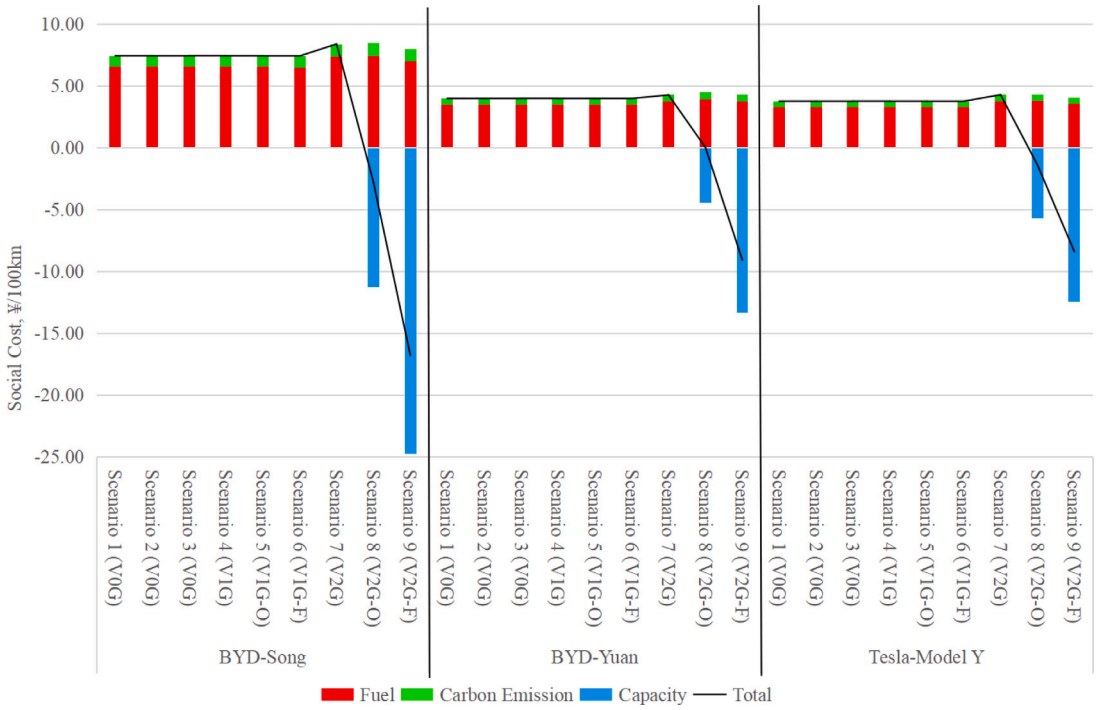

Fig. 6. Social costs of transportation electrification in Gansu Province in 2022.
Notes: The horizontal axis categorizes the three selected EV models under nine distinct (dis)charging scenarios—comprising three unmanaged charging (V0G) scenarios, three smart charging (V1G) scenarios, and three V2G scenarios. The vertical axis measures the social costs in ¥ per 100 km, whereas the different colored bars represent the various cost components that collectively form the social costs. The black curve shows the trend in social costs as the power transfer technologies evolve from V0G to V1G to V2G.

in turn, overall social costs. The magnitude of this effect is considerably larger in Gansu, primarily due to the greater need for dispatchable capacity in high-renewable power systems.

Scenario 9 (V2G-F) leads to a substantial reduction in social costs, primarily by significantly lowering capacity investment needs through higher discharge power during peak-load periods. However, unlike in Guangdong, fast charging in Gansu does not produce additional fuel cost savings relative to regular V2G. This is because Gansu's power system is dominated by a homogeneous coal-fired generation mix, resulting in little variation in marginal fuel costs across different hours. Nevertheless, even without fuel-cost advantages, V2G-F still generates considerable social benefits in Gansu—so much so that the net social cost becomes negative.

These results highlight the importance of designing charging and discharging periods for smart charging and V2G integration. A well-designed schedule can leverage price signals to reduce social costs and provide social benefits.[19] Notably, in July 2024, Gansu province reclassified 6:00-7:00 as the peak period. This adjustment reflects the practical implementation of the insights derived in this study.

Finally, in provinces where renewable energy accounts for a large share of power generation, the electrification of transportation, especially when combined with V2G, not only reduces social costs but also plays a positive role in renewable energy integration. As EV batteries are charged during periods of renewable surplus and discharged during peak-load hours, they function as distributed storage resources that help absorb otherwise-curtailed wind and solar output. To quantify this effect, Appendix A.3 estimates changes in renewable curtailment by comparing the net load with and without EV charging and discharging under each scenario, taking Gansu as a case study. By assessing whether renewable generation exceeds the system's demand or transmission capacity at each hour, the appendix identifies the amount of otherwise curtailed wind and solar energy that could be absorbed through V2G. The results show that V2G substantially reduces renewable energy curtailment in Gansu, where curtailment is driven less by insufficient generation capacity and more by inadequate demand-side flexibility.

7. Mechanism design

Section 6 examines the impact of transportation electrification on the social costs of the power industry and confirms the pivotal role of V2G integration in reducing the social costs. The key to successful V2G deployment is the design of pricing mechanisms that effectively reflect the impact of V2G integration on the social costs in the power industry. These mechanisms are economically efficient because they ensure undistorted price signals.

This section explores two approaches to designing these mechanisms. The first enables EV owners to participate in multiple power markets under V2G integration, thereby optimizing resource allocation through market-driven signals; we refer to this as the "market-driven mechanism". The second approach takes a more direct route by explicitly incorporating all components of the social costs into a comprehensive pricing scheme for V2G integration, which shapes user behavior; we refer to this as the "direct-pricing mechanism". The remainder of this section presents a detailed analysis of each approach.

7.1. Market-driven mechanism

Under the market-driven mechanism, EV owners are encouraged to participate in the electricity spot market through V2G integration.

[19] In fact, if we adjust the charging/discharging schedule assumed in Scenario 7 (see Table 3) by redefining 6:00-7:00 as the discharging period (i.e., classifying it as a peak period), then the social costs will be very close to V2G-O. Similarly, we can anticipate that if we redesign in charging schedule for the unmanaged charging scenarios such that in 6:00-7:00 the EV owners are charging, we would observe much higher social costs compared with those in Fig. 6.

Two key components of the social costs — fuel and carbon emission costs — are reflected in the spot market prices. Moreover, by settling transactions based on Locational Marginal Prices (LMPs) that account for variations in marginal generation and congestion costs across locations, EV owners receive price signals that mirror the broader impacts of transportation electrification on the power system, including not only fuel and carbon emission costs but also transmission congestion costs. During periods of grid congestion, elevated LMPs incentivize EV owners to discharge stored energy, whereas lower LMPs encourage EV charging.

This mechanism also enables EV owners to participate in the capacity market or receive capacity compensation, which reflects the economic impact of V2G integration in reducing capacity investment requirements. The capacity market ensures that the power system maintains adequate generation capacity to meet future demand, and by committing to supplying electricity during peak load periods, EV owners can earn capacity payments that provide an additional revenue stream.

Finally, the mechanism includes access for EV owners to ancillary services markets. Participation in these markets enables EVs to offer essential services — such as frequency regulation, voltage support, and spinning reserves — which are critical for maintaining grid reliability and stability. The integration of EVs into ancillary services markets internalizes the external benefits of V2G integration on ancillary services costs.

In summary, allowing EV owners to engage in the spot, capacity, and ancillary services markets ensures that all components of the social costs are effectively transmitted through market signals. Therefore, this mechanism is considered to yield the first-best outcome.

However, market-driven mechanism faces several challenges. Engaging in multiple markets requires expertise and technical support, which may complicate the participation of EV owners. Market price volatility can lead to inconsistent income streams, potentially dampening enthusiasm for participation. In addition, implementing advanced metering and communication technologies is essential for facilitating real-time data exchange and transaction settlement. To overcome these challenges, the development of intelligent charging and discharging management systems or the promotion of V2G agency services could be instrumental.

7.2. Direct-pricing mechanism

Under the direct-pricing mechanism, EV owners are charged or credited with time-of-use price rates that reflect the social costs imposed on the power industry through transportation electrification. This approach offers several distinct advantages over the market-driven mechanism. It provides clear and straightforward price signals for EV owners, thereby eliminating the need for complex market participation processes and enabling rapid, direct behavioral adjustments based on current cost information.

Furthermore, this direct-pricing mechanism assigns tariffs for charging and discharging, which are explicitly linked to all the relevant components of the social costs. Thus, the social costs of transportation electrification are effectively reflected in prices. Consequently, EV owners can modify their charging and discharging behavior in a transparent pricing environment.

Analyzing data from October 2021 to September 2022 in Guangdong province, Fig. 7 presents the average hourly social costs of transportation electrification under the assumption that each of the three aforementioned EV models charges during specific hours at a regular (dis)charging speed (for more details, see Appendix A.4). Under the direct-pricing mechanism, EV owners are charged or credited based on these rates. For instance, BYD Song users face a charging price of approximately ¥0.9/kWh at 10:00 and could alternatively receive this rate if they opt for discharge. Based on Fig. 7, the maximum annual arbitrage revenue achievable through V2G integration (40% of battery capacity allocated to V2G participation) is estimated at ¥975 for the Tesla Model Y. This revenue can roughly cover the electricity and service costs for a Tesla Model Y to travel 7000–9000 kilometers annually, provided that charging is conducted exclusively during off-peak or shoulder periods.[20]

Notably, the direct-pricing mechanism is also effective for smart charging: lower prices during off-peak hours incentivize EV owners to shift their charging to nighttime, thereby further enhancing grid efficiency and reducing overall social costs. However, the direct-pricing mechanism has some limitations. Price patterns are fixed across days and may fail to fully capture the frequent fluctuations in supply and demand, resulting in suboptimal charging and discharging decisions. Additionally, the mechanism may not provide adequate incentives for EV owners to deliver high-value services during periods of grid stress and relies on advanced metering and communication infrastructure for effective implementation. Therefore, this is considered the second-best mechanism.

8. Conclusions and policy implications

In this study, we quantify the social costs of transportation electrification and evaluate how evolving power-transfer technologies (namely, unmanaged charging, smart charging, and V2G integration) shape these costs across regions with distinct power-system characteristics. The results demonstrate that in region (Guangdong) with low renewable penetration, V2G primarily reduces capacity investment costs to achieve notable social cost reduction and enhances system flexibility; in region (Gansu) with high renewable penetration, it delivers a more substantial reduction in social costs driven by a steeper decline in capacity investment costs and facilitates renewable-energy integration by improving demand-side responsiveness. We further design market-based and direct-pricing mechanisms that internalize these social costs into price signals and provide economically efficient incentives for EV participation.

From a policy perspective, the findings highlight three actionable priorities. First, accelerate the establishment of dynamic, region-specific time-of-use and real-time pricing systems that accurately reflect local load conditions and renewable-energy availability. Aligning tariff structures with actual market-traded load can prevent misaligned incentives and ensure that V2G participation effectively reduces system peaks rather than shifting them. Second, develop integrated market and regulatory frameworks that enable EVs to participate in multiple power markets — spot, capacity, and ancillary services markets — through aggregation platforms or virtual-power-plant operators. Such participation can unlock the full system-level value of distributed storage and generate stable revenue streams for EV owners. Third, strengthen institutional and technological infrastructures for V2G deployment, including interoperable charging standards, data-exchange protocols, and AI-driven energy-management systems. These measures can lower transaction costs, enhance cybersecurity, and improve coordination between grid operators and mobility providers.

[20] We assume a Tesla Model Y with an initial state of charge of 100%. The vehicle owner selects three hours with the highest electricity prices in a day for discharging (17:00–18:00, 19:00–20:00, and 20:00–21:00) with the corresponding electricity price being ¥0.95/kWh for those periods (see Fig. 7). The total discharged electricity is 24 kWh; however, due to power losses, the actual electricity received by the grid is 22.2 kWh. Thus, the revenue from discharging is calculated as $0.95 \times 22.2 = ¥21.09$. Subsequently, the owner will recharge 40% of the discharged electricity during the period with the lowest electricity price of the day, corresponding to 4:00 to 7:00, at ¥0.69/kWh (see Fig. 7). The charging capacity required by the Model Y is 24 kWh, but due to charging losses, the actual electricity consumed is 26.7 kWh, resulting in a charging cost of $0.69 \times 26.7 = ¥18.42$. Based on this, we can calculate the daily arbitrage revenue obtained by the owner through the direct-pricing mechanism to be $21.09 - 18.42 = ¥2.67$. The annual revenue is therefore $2.67 \times 365 = ¥974.55$.

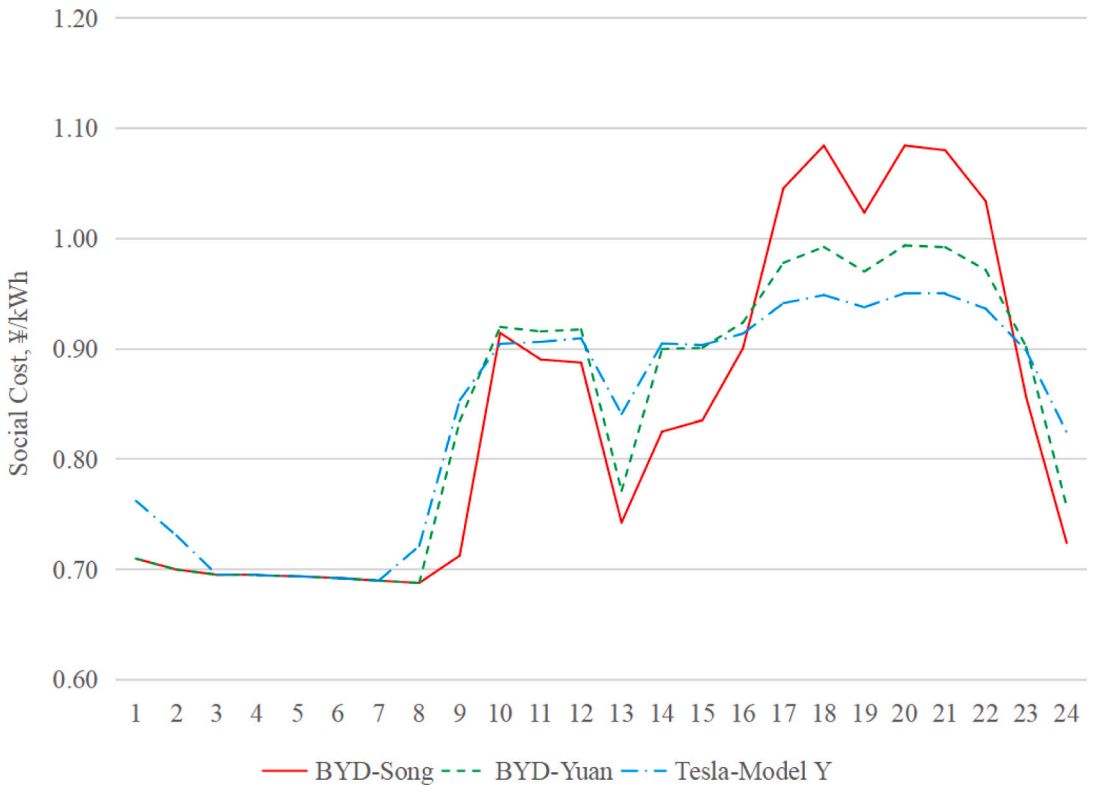

Fig. 7. The direct-price mechanism for V2G integration in Guangdong Province, Oct 2021–Sep 2022.

Looking forward, policy design should move beyond short-term incentives toward long-term governance mechanisms that embed V2G integration into national electrification and carbon-neutrality strategies. Specifically, establishing demonstration zones that couple transportation electrification with renewable-energy bases, refining carbon-pricing schemes to incorporate avoided curtailment benefits, and integrating EV batteries into grid-resilience planning can provide replicable blueprints for large-scale implementation. International collaboration on V2G standards and cross-border electricity trade in the context of electric mobility could further expand the economic and environmental gains identified in this study.

This study also recognizes several limitations and future research directions. First, a deeper understanding of consumer behavior and participation dynamics is essential. User heterogeneity in battery-life concerns, expected returns, and mobility patterns determines the effectiveness of V2G programs. Second, as EV penetration and renewable-energy shares continue to rise, grid-investment requirements and stability constraints warrant further empirical assessment. Finally, integrating AI-enabled forecasting and optimization algorithms into V2G scheduling represents a promising direction for reducing uncertainty and enhancing policy design precision.

CRediT authorship contribution statement

Xuhao Zhan: Writing – original draft, Software, Methodology, Formal analysis, Data curation. **Bowei Guo:** Writing – review & editing, Supervision, Resources, Project administration, Methodology, Funding acquisition, Conceptualization.

Appendices

A.1. The transmission congestion costs and the ancillary services costs

In this section, we incorporate the transmission congestion costs and ancillary services costs arising from transportation electrification into the calculation of social costs in Guangdong and present the specific calculation process.

A.1.1. Estimate the transmission congestion cost

Transmission congestion occurs when the available capacity of the transmission network cannot meet all the demands for electricity transfer. To ensure grid reliability, operators may need to adjust the generation schedules or, in severe instances, reject specific transmission requests, thereby preventing transmission lines from becoming overloaded. Under normal circumstances without congestion, electricity flows freely, resulting in equal nodal prices across interconnected nodes. However, these nodal prices diverge during congestion, reflecting the increased costs associated with grid constraints. Consequently, transportation electrification may exacerbate congestion issues by elevating the electricity load demand, especially during peak hours, whereas V2G integration can help alleviate congestion by incentivizing consumers to shift consumption from peak to off-peak periods.

Although detailed high-frequency congestion cost data for Guangdong are not available publicly, we estimate congestion costs at a 15-min resolution using variations in nodal electricity prices. To achieve this, we utilize spot market data collected from November 2021 to October 2022.[21]

[21] The time period used here is misaligned by one month as the Guangdong electricity spot market did not reach full operation until November 2021.

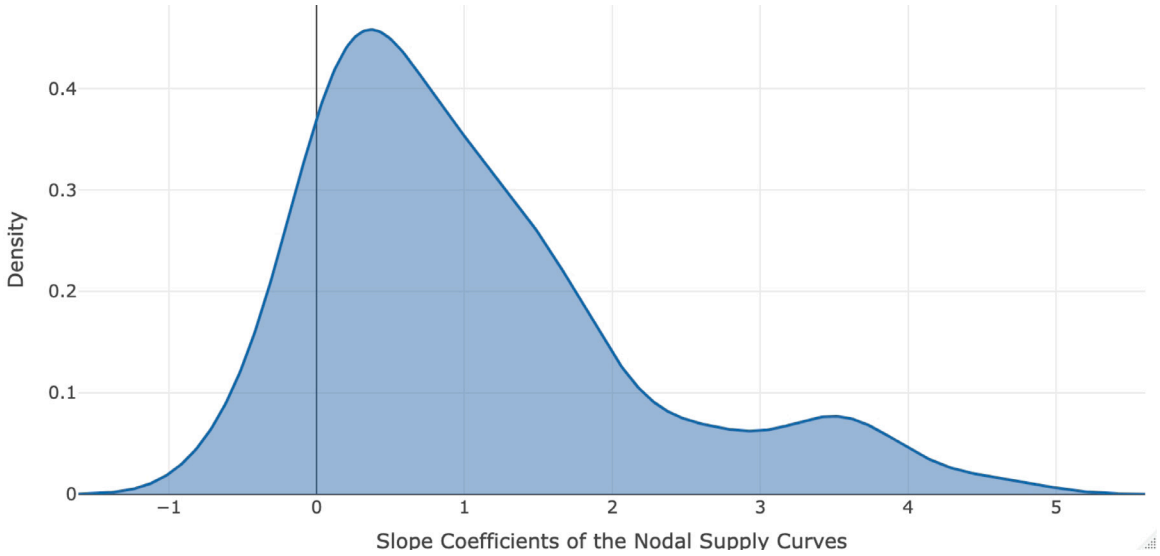

Fig. A.1. Density of the estimated slope coefficients of the nodal supply curves.

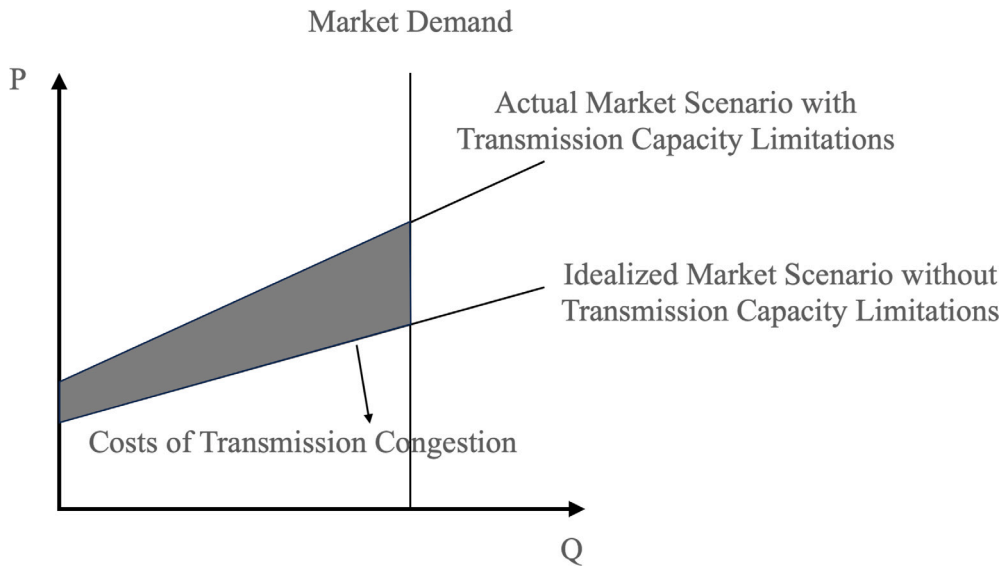

Fig. A.2. Theoretical transmission congestion costs.

In the first step, we align nodal price data with the electricity generation data at the corresponding node and subsequently employ the following instrumental variable (IV) regression models to estimate supply curves for each node—essentially the generators' bidding curves[22]:

$$g_{n,d,h,t} = \gamma_0 + \gamma_{1,n} p_{n,d,h,t} + \theta X_{n,d,h,t} + \epsilon_{n,d,h,t}, \quad \forall n \tag{6}$$

where, n is the generation nodes; $g_{n,d,h,t}$ and $p_{n,d,h,t}$ are the generation and electricity price of node n at time t of hour h on day d, respectively; the vector $X_{n,d,h,t}$ is the control variables, including input costs (coal price, gas price, and carbon emission costs) and time fixed effects (monthly, weekly, and 15-min time dummy variables).

To estimate the supply curve, we employ demand-side shocks as instrumental variables, specifically temperature variations and Guangdong ETS prices. The selection of the *Guangdong* ETS prices is justified by the fact that the province's power industry has been fully integrated into the *national* ETS since July 16, 2021—unlike other sectors, such as cement and steel, which still operate under the provincial ETS. Consequently, fluctuations in Guangdong ETS prices are more likely to affect electricity demand rather than directly impacting electricity supply.

Fig. A.1 presents the density distribution of the estimated slope coefficients of the nodal supply curves. Most of these coefficients are positive, supporting the validity of our estimation methodology. To maintain consistency with economic theory — specifically, the law of supply, which rules out negatively sloped supply curves — we replace negative slope estimates with minimal positive values. Specifically, negative slopes are substituted with 0.001 instead of zero to

Nevertheless, this discrepancy has little impact on our estimation since the data are primarily used to analyze the relationship between electricity load and congestion costs. The derived results are then applied to estimate congestion costs under counterfactual scenarios.

[22] Our analysis concentrates on nodes directly linked to power plants participating in the spot market (generation nodes). Omitting intermediate transmission and distribution nodes is unlikely to significantly distort congestion estimates, as price differentials between generation nodes inherently capture discrepancies involving intervening nodes.

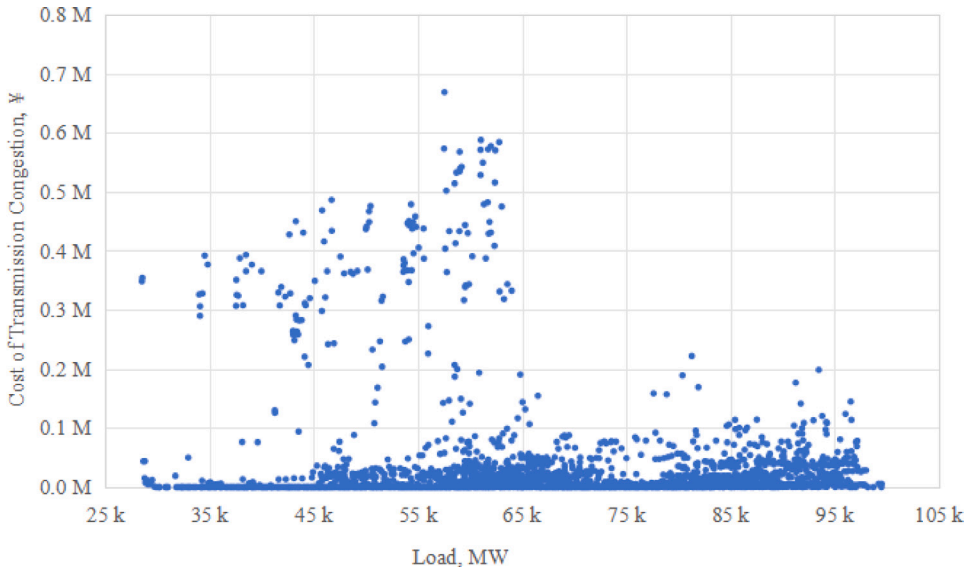

Fig. A.3. Relationships between the costs of transmission congestion and the load in Guangdong, January 2022.

avoid division-by-zero errors during the subsequent calculations. This adjustment implies a near-horizontal supply curve for the nodes.

In the second step, we assume that supply-side shocks affect nodal supply curves through parallel shifts rather than by altering their slopes. Consequently, using the observed nodal prices for each 15-min interval, we identify the supply curves at *each node* and aggregate them into a *market supply curve*. The intersection of this market supply curve and demand represents an idealized scenario of electricity dispatch without transmission capacity constraints. Conversely, by utilizing actual generation data from each node, we construct a realistic market scenario that accounts for limited transmission capacity, potentially leading to congestion. The discrepancy between these idealized and actual market supply scenarios quantifies the transmission congestion costs. Fig. A.2 visually represents this concept under the assumption of inelastic short-run demand. The shaded area in the figure denotes the estimated congestion costs for a given 15-min interval.

In the third step, we model the nonlinear relationship between transmission congestion cost and electricity load. As this relationship is expected to be nonlinear, as shown in Fig. A.3, traditional econometric methods may not accurately capture their relationships. Therefore, this study applies a machine learning method, Support Vector Regression (SVR), to model the nonlinear relationship. Further details are provided in Appendix A.2.

In the fourth step, the counterfactual transmission congestion costs are estimated based on the counterfactual load estimated for different (dis)charging scenarios (recall Section 4.2) using the tuned SVR. Specifically, SVR reveals the relationship between electricity load and transmission congestion cost. As we update the model inputs using the counterfactual load, the outputs are taken as estimates for counterfactual transmission congestion costs.

In the final step, the impact of transportation electrification on transmission congestion cost is estimated using the following formula:

$$S_t = \sum_d \sum_h \sum_t \left[T\left(q'_{d,h,t}, h, t\right) - T\left(q_{d,h,t}, h, t\right) \right] \tag{7}$$

where S_t is the impact of transportation electrification on transmission congestion cost, T is the cost function for transmission congestion, which is nonlinear and depends on the power load and time dummy variables. S_t is estimated using SVR.

A.1.2. Estimate the ancillary services cost

Ancillary services are essential functions that support the stability and reliability of power grid operations. These include maintaining a balance between electricity supply and demand, regulating voltage and frequency, and rapidly restoring services after disruptions. Transportation electrification is expected to increase ancillary services costs as it introduces additional volatility into electricity load patterns. This increased variability makes maintaining a balance between supply and demand more challenging, potentially destabilizing grid operations.

High-frequency data on ancillary services costs are not publicly accessible for Guangdong province. However, its electricity spot market incorporates both day-ahead and real-time markets without an intermediate intraday market. Consequently, the real-time market serves as an effective balancing mechanism. This market structure allows us to estimate a significant portion of ancillary services cost — specifically, the energy imbalance cost — by taking the product of price differences (between day-ahead and real-time market) and the corresponding load differences.

Unfortunately, our existing dataset does not allow us to estimate other ancillary services components, such as frequency and voltage regulation or rapid system recovery after disturbances. However, considering that energy imbalance costs typically represent around 40% of total ancillary services cost — according to data from PJM[23] — we scale our calculated energy imbalance costs by dividing them by 0.4 to estimate the total ancillary services expenses. Using this method, we estimate Guangdong's ancillary services cost to be approximately ¥0.57 cent/kWh (or $0.08 cent/kWh) during our one-year sample period. This estimate aligns reasonably with the average ancillary services cost of $0.11 cent/kWh reported by PJM from 2019 to 2021. Given that Guangdong has a significantly lower renewable energy penetration than PJM, its actual ancillary services cost is expected to be correspondingly lower.

Subsequently, in accordance with the third, fourth, and fifth steps for estimating the transmission congestion cost, we apply SVR to model the relationship between ancillary services cost and electricity load. Fig. A.4 shows that this relationship is nonlinear too. Then we use the tuned SVR to estimate the counterfactual ancillary services costs. Finally, we use the following formula to estimate the impact of transportation electrification on ancillary services cost:

$$S_a = \sum_d \sum_h \sum_t \left[A\left(q'_{d,h,t}, h, t\right) - A\left(q_{d,h,t}, h, t\right) \right] \tag{8}$$

[23] See http://www.monitoringanalytics.com/reports/PJM_State_of_the_Market/2022/2022-som-pjm-vol2.pdf.

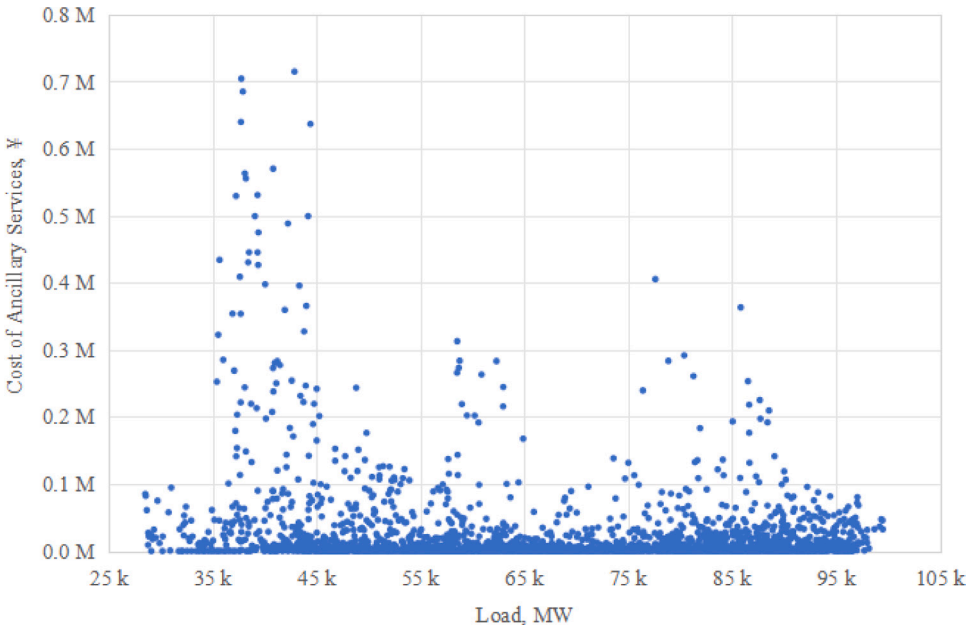

Fig. A.4. Relationships between the costs of ancillary services and the load in Guangdong, January 2022.

where S_a is the impact of transportation electrification on ancillary services cost, estimated by using SVR. A is the nonlinear cost function for ancillary services depending on the power load and time dummy variables.

A.1.3. Result

Table A.1 presents the impact of transportation electrification on the transmission congestion costs and ancillary services costs in Guangdong's power industry under the nine proposed scenarios, based on a dataset spanning October 2021 to September 2022.

Overall, there is a declining trend of transmission congestion costs when moving from the V0G scenarios to V1G and further to V2G, validating that appropriate charging and discharging behaviors can, to a certain extent, alleviate power transmission congestion. However, such a downward trend is not evident in the ancillary services costs. This discrepancy may stem from the fact that our estimation of the ancillary services costs is mainly based on the calculation of imbalance costs, which leads to a certain gap between the estimated value and the actual ancillary services costs. Nevertheless, as reflected in the data across all scenarios, both costs remain at a very low level relative to the social costs, with the transmission congestion costs accounting for <1.1%, the ancillary services costs <0.8%, and their total share not exceeding 1.3%. Therefore, the potential estimation error in the ancillary services costs can be negligible relative to the overall social costs.

Notably, our estimates of transmission congestion costs and ancillary services costs focus exclusively on the short-term impacts associated with transportation electrification. Specifically, we evaluate immediate and direct effects while excluding longer-term considerations such as changes to investment decisions in transmission and distribution infrastructure and ancillary services facilities. However, it is important to recognize that long-term investment decisions are inherently linked to short-term benefits. Specifically, in equilibrium, where marginal costs are equal to marginal benefits, the short-term impacts identified in this analysis effectively represent the annual cash flows necessary to sustain long-term investments.

Table A.1
Transmission congestion costs and ancillary services costs in Guangdong (Oct 2021–Sep 2022).

Scenario	T.C. Cost	A.S. Cost	Social cost
BYD-Song (Unit: ¥/100 km)			
Scenario 1 (V0G)	0.1789	0.0058	17.3467
Scenario 2 (V0G)	0.1750	0.0577	28.8203
Scenario 3 (V0G)	0.0793	0.0106	17.3315
Scenario 4 (V1G)	0.0574	0.0532	16.5766
Scenario 5 (V1G-O)	0.0429	0.0529	16.4983
Scenario 6 (V1G-F)	0.0132	0.0616	16.4516
Scenario 7 (V2G)	0.0197	0.0471	8.6875
Scenario 8 (V2G-O)	0.0290	0.1386	8.6276
Scenario 9 (V2G-F)	−0.0345	0.0206	−5.1923
BYD-Yuan (Unit: ¥/100 km)			
Scenario 1 (V0G)	0.1004	−0.0024	9.3469
Scenario 2 (V0G)	0.0802	0.0092	13.8775
Scenario 3 (V0G)	0.0414	0.0051	9.2027
Scenario 4 (V1G)	0.0291	0.0269	8.8843
Scenario 5 (V1G-O)	0.0291	0.0269	8.8843
Scenario 6 (V1G-F)	0.0071	0.0331	8.8385
Scenario 7 (V2G)	0.0120	0.0086	5.9284
Scenario 8 (V2G-O)	0.0282	0.0677	5.9309
Scenario 9 (V2G-F)	−0.0185	0.0112	−2.8447
Tesla-Model Y (Unit: ¥/100 km)			
Scenario 1 (V0G)	0.0905	0.0034	8.7871
Scenario 2 (V0G)	0.0891	0.0298	14.6548
Scenario 3 (V0G)	0.0401	0.0051	8.7839
Scenario 4 (V1G)	0.0292	0.0269	8.3989
Scenario 5 (V1G-O)	0.0216	0.0270	8.3591
Scenario 6 (V1G-F)	0.0066	0.0310	8.3347
Scenario 7 (V2G)	0.0188	0.0112	4.5003
Scenario 8 (V2G-O)	0.0155	0.0696	4.4363
Scenario 9 (V2G-F)	−0.0173	0.0105	−2.5095

Notes: "T.C. Cost" refers to transmission congestion cost, "A.S. Cost" to ancillary services cost, and "Social Cost" is the sum of fuel cost, carbon emission cost, and capacity investment cost.

A.2. Support Vector Regression (SVR)

We utilize Support Vector Regression (SVR) to investigate the relationship between the transmission congestion costs and ancillary services costs and electricity load for several reasons: First, the relationship between these two variables typically exhibits complex nonlinear characteristics, and SVR excels at modeling such nonlinearities effectively through its kernel functions, while mitigating the risks of overfitting. Second, compared to alternative methods, such as deep neural networks or random forests, SVR demonstrates strong predictive

performance and generalization capability even with limited sample sizes, making it particularly suitable given our dataset's moderate scale. Moreover, SVR models are computationally efficient, involve fewer parameters, and are easier to tune and interpret, thereby enhancing their applicability in practical contexts.

Notably, we use real-time load (see Table 1) and monthly, weekly, and 15-minute time dummies as the feature vectors/inputs for the model training set, and take the actual transmission congestion costs and ancillary services costs, estimated using the methods in Appendices A.1.1 and A.1.2, as the labels/outputs. In the prediction set, we use the counterfactual loads of the nine scenarios as inputs, while the outputs are taken as estimates for counterfactual transmission congestion costs and ancillary services costs.

The basic idea of SVR is to map the data to a high-dimensional feature space through a nonlinear mapping and perform linear regression in this space. The SVR model is developed from the optimal classification surface in the linearly separable case. An epsilon-insensitive loss function is introduced to ensure the sparsity of the dual variables and to optimize the generalization capability of the model. The optimization problem of SVR is formulated as follows:

$$\min_{w,b} \frac{1}{2}\|w\|^2 + C\sum_{i=1}^{n}(\xi_i + \xi_i^*)$$
$$\text{s.t.} \quad \begin{cases} (w \cdot x_i + b) - y_i \le \epsilon + \xi_i \\ y_i - (w \cdot x_i + b) \le \epsilon + \xi_i^* \\ \xi_i, \xi_i^* \ge 0 \end{cases} \quad \forall i \tag{9}$$

Given the training data $\{(x_i, y_i) \,|\, x_i \in \mathbb{R}^d, y_i \in \mathbb{R}, i = 1, 2, \ldots, n\}$ satisfying $f(x_i) = w \cdot x_i + b$, where $f(x)$ is the SVR model, w is the weight vector, and b is a constant threshold. ξ_i and ξ_i^* are slack variables introduced due to the error in fitting in the optimization problem, C is the cost parameter determining the trade-off between achieving a low training error and a low capacity of the decision function, ϵ is the tolerance deviation (epsilon-insensitive tube), which is used to control the range of regression errors, thus affecting the number of support vectors and the generalization ability of the model. In our analysis, y_i is either the transmission congestion cost or the ancillary services cost, whereas x_i is the electricity load.

The Lagrange function is introduced for the optimization problem above:

$$L(w, b, \xi, \xi^*, \alpha, \alpha^*, \gamma, \gamma^*) = \frac{1}{2}\|w\|^2 + C\sum_{i=1}^{n}(\xi_i + \xi_i^*) - \sum_{i=1}^{n}\gamma_i\xi_i - \sum_{i=1}^{n}\gamma_i^*\xi_i^* + \sum_{i=1}^{n}\alpha_i[(w \cdot x_i + b) - y_i - \epsilon - \xi_i] + \sum_{i=1}^{n}\alpha_i^*[y_i - (w \cdot x_i + b) - \epsilon - \xi_i^*] \tag{10}$$

where $\alpha, \alpha^*, \gamma, \gamma^*$ are the Lagrange multipliers that satisfy $\alpha, \alpha^*, \gamma, \gamma^* \ge 0$. Exploiting the Karush Kuhn Tucker (KKT) conditions, taking the partial derivatives of $L(w, b, \xi, \xi^*, \alpha, \alpha^*, \gamma, \gamma^*)$ with respect to w, b, ξ and ξ^*, respectively, and setting them equal to 0 to estimate w, b, ξ and ξ^*:

$$\begin{cases} \frac{\partial L}{\partial w} = w + \sum_{i=1}^{n}(\alpha_i - \alpha_i^*)x_i = 0 \\ \frac{\partial L}{\partial b} = \sum_{i=1}^{n}(\alpha_i - \alpha_i^*) = 0 \\ \frac{\partial L}{\partial \xi_i} = C - \gamma_i - \alpha_i = 0 \\ \frac{\partial L}{\partial \xi_i^*} = C - \gamma_i^* - \alpha_i^* = 0 \end{cases} \quad \forall i \tag{11}$$

The dual form of the optimization problem is obtained by substituting the estimation into L. Using the kernel function $\kappa(x_i, x_j) = \phi(x_i)^T\phi(x_j)$, the inner product in the high-dimensional feature space can be converted into a calculation of the kernel function in the input space, thus indirectly realizing the mapping from the input space to the high-dimensional feature space. At this time, the dual-optimization problem is expressed as:

$$\max_{\alpha,\alpha^*} \sum_{i=1}^{n}[y_i(\alpha_i^* - \alpha_i) - \epsilon(\alpha_i^* + \alpha_i)] - \frac{1}{2}\sum_{i=1}^{n}\sum_{j=1}^{n}(\alpha_i^* - \alpha_i)(\alpha_j^* - \alpha_j)\kappa(x_i, x_j)$$
$$\text{s.t.} \quad \begin{cases} \sum_{i=1}^{n}(\alpha_i - \alpha_i^*) = 0 \\ 0 \le \alpha, \alpha^* \le C \end{cases} \quad \forall i \tag{12}$$

By solving the dual problem according to the KKT conditions, the optimal regression function form can be obtained as follows:

$$f(x) = \sum_{i=1}^{n}(\alpha_i - \alpha_i^*)\kappa(x_i, x) + b \tag{13}$$

The stability and accuracy of the SVR model largely depend on the choice of kernel function, hyperparameters, and penalty terms (Wu et al., 2009). In particular, SVR maps data from the input space to the feature space through a nonlinear function called the kernel function to perform nonlinear regression. Therefore, to improve the performance of SVR, the best combination of parameters needs to be selected for the model.

In practice, hyperparameters such as the cost parameter C and tolerance deviation parameter ϵ need to be optimized to achieve the best performance of the model. This process is called hyperparameter optimization or model selection. In this study, SVR hyperparameter selection is performed through a grid search, which is a standard SVR hyperparameter optimization method. Specifically, a large number of models are trained for different parameter combinations and the model with the smallest error is selected as the optimal result based on indicators such as the root mean square error (RMSE).

A.3. Reduction in renewable curtailments in Gansu province

This section provides a first-order, order-of-magnitude estimation of the impact of V2G on reducing renewable energy curtailment, taking Gansu Province as a case study. Because detailed operational data for curtailment are not publicly available, we conduct a methodologically consistent sensitivity analysis using 15-minute wind, solar, and total electricity generation data for 2022. Rather than aiming for a full power-system dispatch simulation, this analysis offers a transparent and analytically tractable approximation that quantifies the plausible magnitude of Gansu's curtailment and the incremental effect that V2G could deliver. This approach is consistent with prior studies that adopt simplified empirical representations when detailed operational constraints are unavailable (Newbery, 2023; Newbery and Biggar, 2024; Newbery, 2025).

At each 15-minute interval, curtailment is defined as the difference between the potential renewable output (i.e., the renewable generation that would be produced absent any grid-imposed restrictions) and the actual generation. In principle, curtailment would occur only when potential renewable production exceeds contemporaneous electricity demand. In practice, however, power-system operators often curtail before reaching this physical limit. This reflects a widely observed operational practice: because large swings in wind and solar output can challenge frequency regulation and ramping capability, system operators typically enforce an implicit renewable penetration threshold beyond which additional renewable injections are curtailed for system-security reasons. Newbery (2023) documents this behavior in high-renewable systems. Following this empirical insight, we adopt a simplified representation in which curtailment is triggered whenever the real-time renewable share exceeds a threshold β. This assumption does not aim to replicate full system-operation detail but rather provides a behaviorally consistent approximation of curtailment onset.

Newbery (2021) first discussed how renewable energy curtailment rates are influenced by Simultaneous Non-Synchronous Penetration (SNSP, the share of non-synchronous generation, specifically wind and

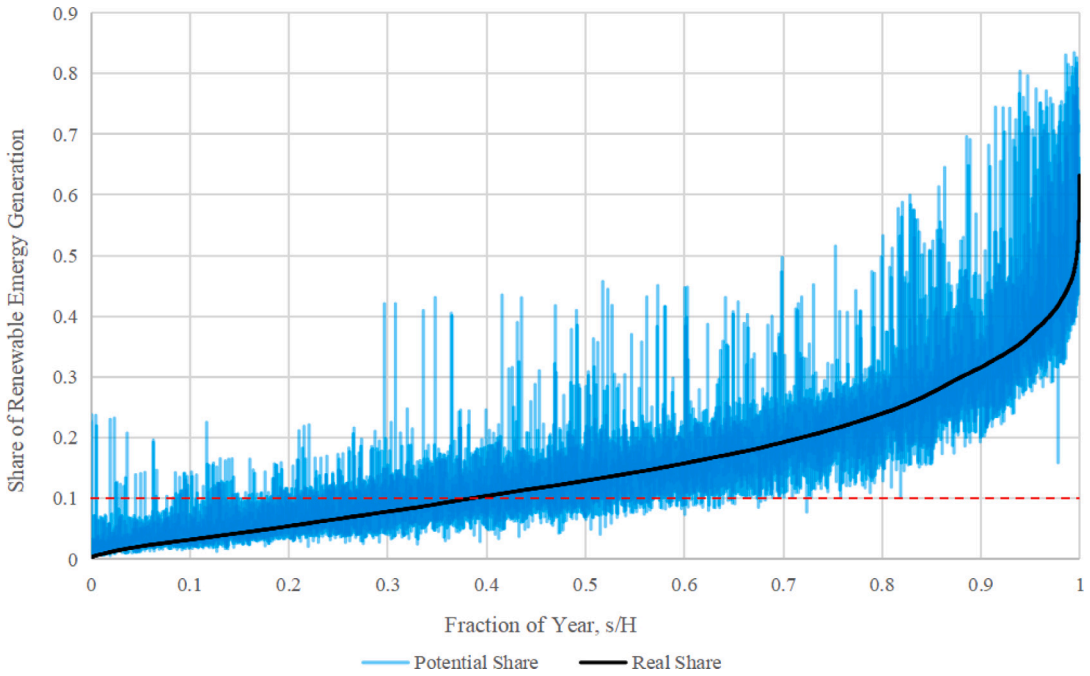

Fig. A.5. Renewable energy generation share curve in Shandong Province in 2022.
Notes: We sort the share of actual grid-connected renewable energy in Shandong in ascending order to form the black curve in this figure. The blue curve represents the proportion of potential renewable energy generation at the same sorted moments. Theoretically, the difference between the two curves indicates the proportion of curtailment in total generation. It is noted that there are cases where the proportion of potential renewable energy generation is lower than that of actual grid-connected energy in the figure, mainly attributed to prediction errors, as the potential renewable energy generation is forecasted on the morning one day in advance.

solar PV, similar to the definition of β in this study). Specifically, non-synchronous generation connects directly to the grid without rotating machinery and therefore does not provide inertia for maintaining system frequency. As a result, SNSP is subject to an operational threshold, beyond which system stability is threatened. Newbery's study shows that curtailment declines as SNSP increases. In the Single Electricity Market (SEM) of the island of Ireland, SNSP levels are relatively high due to substantial installed wind capacity—a condition not yet observed in China.

Fig. A.5 presents potential and actual grid-connected renewable energy in Shandong Province, a Chinese system with relatively high renewable penetration similar to Gansu.[24] It shows that once the actual grid-connected share approaches roughly 10%, potential renewable production rises sharply, leading to more pronounced curtailment.

It is important to acknowledge that neither Ireland nor Shandong perfectly represents Gansu's system conditions. Their renewable penetration structures, operational constraints, and system security requirements differ from those of Gansu, and therefore cannot be mapped directly. To account for this uncertainty, we adopt a range of renewable penetration thresholds rather than relying on a single empirical benchmark. Lower values of β provide a conservative lower bound consistent with today's system flexibility in Gansu, while higher values reflect possible improvements in grid strength, flexibility, and stability as China's power system modernizes.

For this reason, and to ensure that our conclusions are robust to alternative operational assumptions, we evaluate the impact of EV integration on curtailment mitigation under four threshold levels: β = 0.1, 0.2, 0.3, and 0.4.[25]

Let $f(t)$ denote the realized renewable share in 15-minute interval t, and let $k(t)$ denote the curtailment volume. Under this representation, curtailment occurs whenever $f(t) \geq \beta$. For analytical convenience, we reorder the sequence of shares to obtain a nondecreasing series $f(s)$, where s indexes the ordered 15-minute intervals. In this ordering, $s = 1$ corresponds to the lowest renewable share observed in 2022, and the threshold β partitions the series into intervals with and without curtailment.

Fig. A.6 plots the reordered series $f(s)$, the empirical distribution of real-time renewable generation shares in Gansu in 2022. The curve exhibits an approximately linear pattern over most of its support, with only mild deviations at the extremes. Motivated by this empirical regularity, we model the reordered renewable share using a simple linear approximation:

$$f(s) = \alpha_0 + \alpha_1 \frac{s}{H} \tag{14}$$

where H is the total number of 15-minute intervals in the year (i.e., $H = 35{,}040$). Under the threshold representation introduced above, curtailment begins at the first index s^*, satisfying $f(s^*) = \beta$. Solving the linear expression yields $s^* = \frac{\beta-\alpha_0}{\alpha_1} H$, implying that renewable penetration exceeded the threshold in $1 - \frac{\beta-\alpha_0}{\alpha_1}$ of the year.

The potential renewable generation share, defined as the ratio of the sum of realized and curtailed renewable output to total electricity generation, does not typically exhibit a linear relationship with the reordered index s. Empirical evidence from high-renewable regions such as California suggests that the potential share tends to increase in a convex or exponential pattern as renewable availability rises.[26] Fig. A.7 illustrates the conceptual mapping between the empirical renewable

[24] The data come from the authors' ongoing research.

[25] If a larger value of β is set, Gansu Province would have experienced renewable energy curtailment in a small fraction of year in 2022 (if β = 0.5, then the proportion of 15-minute intervals with renewable energy curtailment is 5%), which is inconsistent with facts. Therefore, we set the maximum β at 0.4, corresponding to a curtailment occurrence in 25% of the year, and use this as the lower bound for evaluating the marginal impact of electric vehicles on reducing renewable energy curtailment.

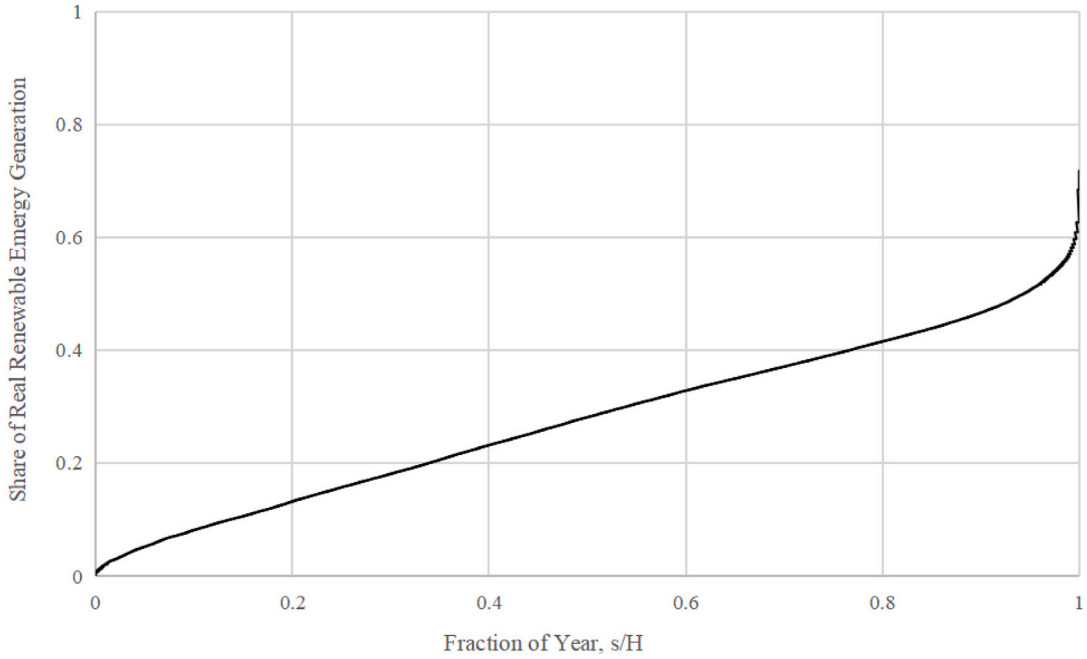

Fig. A.6. Real renewable energy generation share curve in Gansu Province in 2022.

share $f(s)$ and its hypothetical potential counterpart. In this diagram, segment *AB* represents the reordered actual renewable share $f(s)$, while curve *OC* represents the potential share in the absence of curtailment. The two curves intersect at point *E*, which corresponds to the threshold index s^*, where curtailment begins.

For tractability, we approximate the potential share curve by a linear segment *ED* over the domain $s \in [s^*, H]$. This approximation retains the essential geometric feature that the potential share grows faster than the realized share in the curtailment region. Formally, we represent the potential share by:

$$g(s) = \beta + \gamma_1 \frac{s - s^*}{H}, \quad s \geq s^* \tag{15}$$

where $\gamma_1 > \alpha_1$ ensures that $g(s)$ lies above $f(s)$ in the curtailment region. This linearization provides a transparent and reproducible way to approximate potential renewable availability without materially affecting the marginal effect of V2G at the single-vehicle scale.

The purpose of this approximation is to generate a tractable estimate of curtailment volumes rather than to simulate full-system dispatch. Under this objective, the linear representation of the potential share $g(s)$ is sufficient because the results depend only on the difference between potential and realized renewable availability, not on the precise curvature of the potential curve. Accordingly, the curtailment volume at each reordered intervals is computed as:

$$k(s) = \begin{cases} 0, & s < s^* \\ W(s) \cdot \frac{g(s)}{f(s)} - W(s), & s \geq s^* \end{cases} \tag{16}$$

where $W(s)$ denotes the realized renewable generation in interval s. The term $W(s) \cdot \frac{g(s)}{f(s)}$ represents the counterfactual renewable output that would have been generated absent curtailment, and the difference yields the curtailed volume.

Summing over all intervals gives the total curtailment in Gansu during 2022:

$$K = \sum_{s=0}^{H} k(s), \quad H = 35,040 \tag{17}$$

[26] Source: https://www.caiso.com/about/our-business/managing-the-evolving-grid.

Given the observed series $f(s)$ and the threshold β, the total volume uniquely pins down the slope parameter γ_1 of the potential share curve *ED* in Fig. A.7. With γ_1 determined, the full sequence of curtailed volumes $k(s)$ is obtained, and mapping the reordered index s back to the original time index t yields the curtailment time series at 15-minute resolution.

The effect of V2G integration on renewable energy curtailment in Gansu province depends on the number of quarter-hours in which excessive renewable energy generation needs to be curtailed while EVs are charging. This is quantified using the following equation:

$$G_k = \sum_d \sum_h \sum_t \{ \left(q'_{d,h,t} - q_{d,h,t} \right) I_{k(t) \geq \left(q'_{d,h,t} - q_{d,h,t} \right)} + k(t) I_{k(t) < \left(q'_{d,h,t} - q_{d,h,t} \right)} \} \tag{18}$$

where G_k is the impact of transportation electrification on renewable energy curtailment. I_A is a binary variable with $A \in \{ k(t) > \left(q'_{d,h,t} - q_{d,h,t} \right), k(t) < \left(q'_{d,h,t} - q_{d,h,t} \right) \}$, indicating whether the curtailed renewable is sufficient for the excess load demand from transportation electrification. If A is true at time t of hour h on day d, $I_A = 1$; otherwise, $I_A = 0$.

Subsequently, we analyze the impact of transportation electrification on renewable energy curtailment across the nine (dis)charging scenarios in Gansu in 2022 outlined in Section 4.2. Notably, for the convenience of presentation, only the results of Scenario 1 (V0G, charging begins at 08:00), Scenario 5 (Optimal V1G), and Scenario 8 (Optimal V2G) are presented here as the representative scenarios for V0G, V1G, and V2G, respectively.

Fig. A.8 illustrates the results. Overall, transportation electrification reduces renewable energy curtailment across all scenarios, with Optimal V2G integration (Scenario 8) delivering the most substantial benefits. This outcome is primarily due to the optimal alignment of V2G charging and discharging schedules with periods of high surplus generation. Additionally, as the threshold β for curtailment initiation increases, the marginal impact of EVs gradually diminishes. This is because a higher threshold indicates that curtailment occurs in more concentrated time periods with less severe curtailment overall, leaving less room for EVs to mitigate curtailment.

Specifically, under the scenario of $\beta = 0.3$, curtailment occurred in 45% of the 15-minute intervals. At this point, for every additional

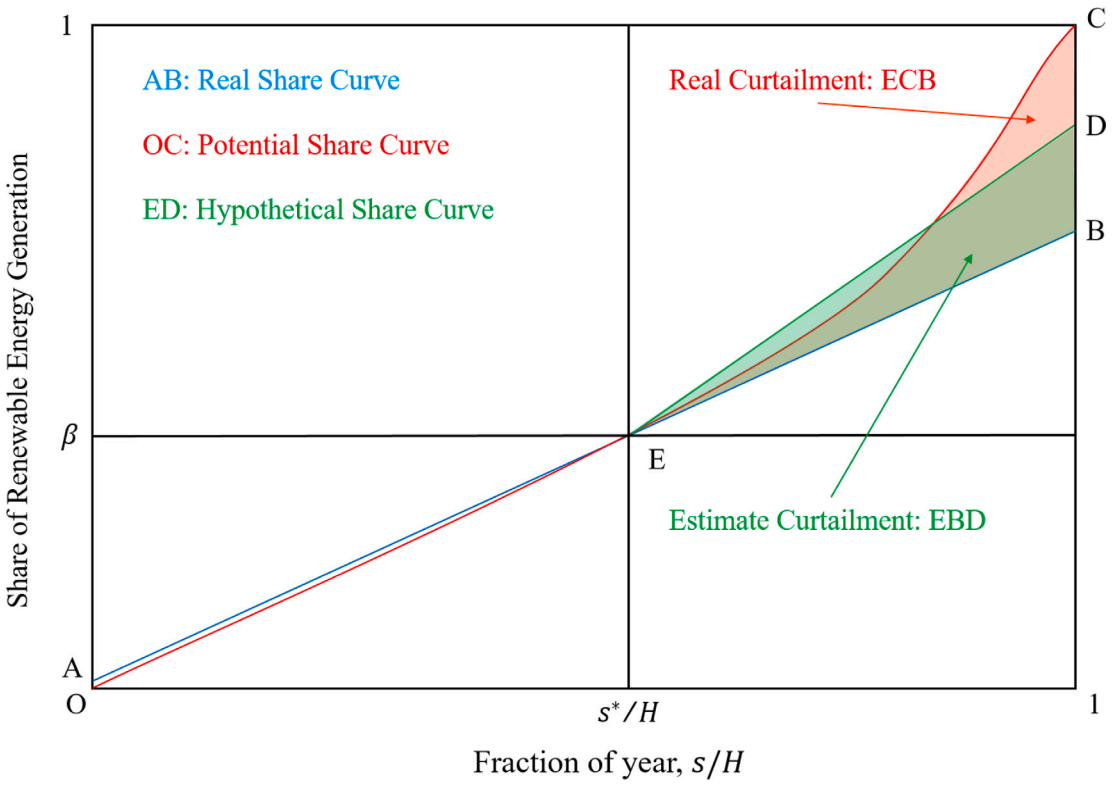

Fig. A.7. Geometric illustration of renewable energy curtailment.

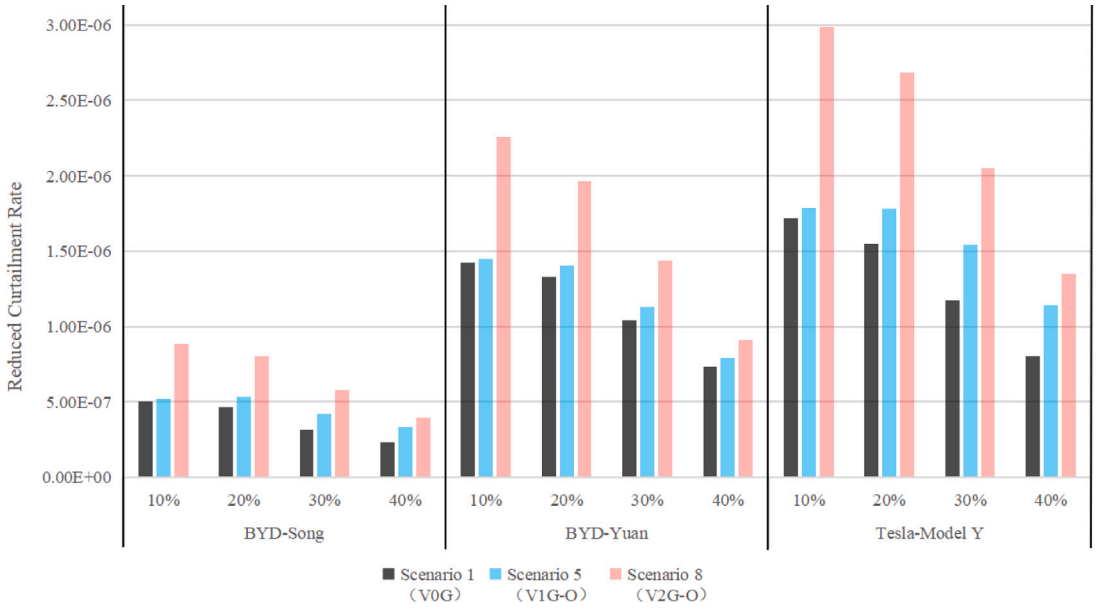

Fig. A.8. Reduced curtailment rate from a single EV in Gansu Province in 2022.
Notes: The horizontal axis delineates three scenarios corresponding to different thresholds of renewable energy curtailment across the three EV models, whereas the vertical axis represents the change in the curtailment rate per EV.

1000 T Model Y adopting V2G integration, the renewable energy curtailment rate decreases by 0.20%, which are 0.05% and 0.09% greater, respectively, than those achieved through Optimal V1G (Scenario 5) and V0G (Scenario 1). Given the 2022 renewable energy curtailment rates of 4.8% in Gansu, zero curtailment may be achieved with the deployment of 24,000 T Model Y vehicles under V2G integration.

Scenario 1 schedules charging during the interval from 13:00 to 15:00—precisely when Gansu's renewable generation peaks and the market-traded load approaches its minimum (recall Fig. 3(b)). During this period, an increase in electricity demand is expected to reduce curtailment, as highlighted by Novan and Wang (2024). Consequently, even unmanaged charging in these scenarios can achieve a reduction in renewable curtailment comparable to that of optimal smart charging (Scenario 5).

Finally, EVs with larger battery capacities (i.e., Tesla Model Y in our case) more effectively reduce renewable energy curtailment,

Table A.2
Thermal efficiency and emission factors for different fossil Plants in Guangdong.

Variable	Unit	Coal plants			Gas turbines	
		Large	Middle	Small	Double-shaft	Single-shaft
Thermal Efficiency	%	42.30	38.45	36.00	47.40	51.10
Emission Factors	tCO_2/MWh	0.729	0.800	0.859	0.396	0.366

Notes: The data are sourced from the South China Regulatory Office of the National Energy Administration. The original data includes the thermal efficiency of each power plant. This table represents the average characteristics of power plants in October 2021 and excludes power plants retired before or put into use after this time.

Table A.3
Social costs of transportation electrification in Guangdong Province (Oct 2021–Sep 2022).

Scenario	Fuel	Carbon	Capacity	Social cost
BYD-Song (Unit: ¥/100 km)				
Scenario 1 (V0G)	16.4297	0.9170	0.0000	17.3467
Scenario 2 (V0G)	16.6511	0.9102	11.2590	28.8203
Scenario 3 (V0G)	16.4126	0.9189	0.0000	17.3315
Scenario 4 (V1G)	15.6290	0.9476	0.0000	16.5766
Scenario 5 (V1G-O)	15.5468	0.9515	0.0000	16.4983
Scenario 6 (V1G-F)	15.4972	0.9544	0.0000	16.4516
Scenario 7 (V2G)	17.8601	1.0627	−10.2353	8.6875
Scenario 8 (V2G-O)	17.7834	1.0795	−10.2353	8.6276
Scenario 9 (V2G-F)	16.2865	1.0388	−22.5176	−5.1923
BYD-Yuan (Unit: ¥/100 km)				
Scenario 1 (V0G)	8.8553	0.4916	0.0000	9.3469
Scenario 2 (V0G)	8.9368	0.4896	4.4512	13.8775
Scenario 3 (V0G)	8.7051	0.4977	0.0000	9.2027
Scenario 4 (V1G)	8.3741	0.5102	0.0000	8.8843
Scenario 5 (V1G-O)	8.3741	0.5102	0.0000	8.8843
Scenario 6 (V1G-F)	8.3257	0.5128	0.0000	8.8385
Scenario 7 (V2G)	9.4101	0.5648	−4.0465	5.9284
Scenario 8 (V2G-O)	9.4075	0.5700	−4.0465	5.9309
Scenario 9 (V2G-F)	8.7374	0.5574	−12.1395	−2.8447
Tesla-Model Y (Unit: ¥/100 km)				
Scenario 1 (V0G)	8.3225	0.4645	0.0000	8.7871
Scenario 2 (V0G)	8.4355	0.4612	5.7581	14.6548
Scenario 3 (V0G)	8.3185	0.4655	0.0000	8.7839
Scenario 4 (V1G)	7.9189	0.4800	0.0000	8.3989
Scenario 5 (V1G-O)	7.8771	0.4820	0.0000	8.3591
Scenario 6 (V1G-F)	7.8511	0.4836	0.0000	8.3347
Scenario 7 (V2G)	9.1394	0.5432	−5.1823	4.5003
Scenario 8 (V2G-O)	9.0687	0.5499	−5.1823	4.4363
Scenario 9 (V2G-F)	8.2700	0.5273	−11.3069	−2.5095

Notes: Here, "Fuel" refers to the fuel cost, "Carbon" to the social cost of carbon emissions, "Capacity" to the generation capacity investment cost; and "Social Cost" is the sum of these three costs.

with the additional storage capacity increasing electricity demand and enhancing grid balancing.

A.4. Direct-price mechanism design

To ensure economic efficiency, the tariffs paid or received by EV owners under V2G integration should accurately reflect the incremental social costs imposed on the power industry by transportation electrification. Section 5 details the methodology employed to estimate the social costs. Building on this foundation, we quantify the hourly impact of EV charging on social costs and provide a precise basis for setting tariff rates. By aligning these hourly price signals directly with the underlying social costs, we can ensure that EV owners face appropriate economic incentives, thereby promoting efficient resource allocation within the electricity market.

To estimate hourly social costs, we assume that one million EVs are simultaneously charged during each of the 8760 h throughout the sample period (October 2021 to September 2022).[27] Subsequently, the hourly social costs are summed across all days, averaged over the total number of days in the year (365 days), and finally divided by the total charging load for each hour to derive the social costs per unit of electricity consumed (¥/kWh).

In the main context, capacity investment costs measure the additional generation capacity required during peak hours under different scenarios. However, when estimating hourly social costs, it is crucial to note that generation capacity investments made during peak hours simultaneously satisfy the capacity requirements for all other hours. Thus, instead of attributing capacity investment costs exclusively to peak-load hours, these costs are distributed across all 24 h, based on each hour's relative contribution to incremental capacity needs. Specifically, the daily capacity investment cost is allocated to each hour using the following weighted formula:

$$S_k^{i,\text{new}} = \frac{S_k^{i,\text{old}}}{\sum_{j=1}^{24} S_k^{j,\text{old}}} \cdot \max_{j=1,\ldots,24} S_k^{j,\text{old}}, \quad i = 1, 2, \ldots, 24 \tag{19}$$

[27] One million EVs are chosen rather than a single vehicle because a single vehicle only induces additional capacity investment costs during the peak-load hour. However, transportation electrification can shift the daily peak-load hour and consequently create capacity investment costs at additional time intervals. In 2024, approximately 2.89 million new-energy vehicles were registered in Guangdong province (source: https://www.gd.gov.cn/gdywdt/bmdt/content/post_4422331.html). Thus, our assumption of one million vehicles is a realistic scaling to reflect the aggregated impact.

Table A.4
Social costs of transportation electrification in Gansu Province in 2022.

Scenario	Fuel	Carbon	Capacity	Social cost
BYD-Song (Unit: ¥/100 km)				
Scenario 1 (V0G)	6.5376	0.9099	0.0000	7.4475
Scenario 2 (V0G)	6.5363	0.9077	0.0000	7.4440
Scenario 3 (V0G)	6.5447	0.9089	0.0000	7.4537
Scenario 4 (V1G)	6.5357	0.9099	0.0000	7.4456
Scenario 5 (V1G-O)	6.5312	0.9083	0.0000	7.4395
Scenario 6 (V1G-F)	6.5267	0.9077	0.0000	7.4343
Scenario 7 (V2G)	7.3734	1.0272	0.0000	8.4006
Scenario 8 (V2G-O)	7.4343	1.0343	−11.2554	−2.7868
Scenario 9 (V2G-F)	7.0053	0.9741	−24.7620	−16.7826
BYD-Yuan (Unit: ¥/100 km)				
Scenario 1 (V0G)	3.5113	0.4885	0.0000	3.9998
Scenario 2 (V0G)	3.5129	0.4875	0.0000	4.0004
Scenario 3 (V0G)	3.5165	0.4891	0.0000	4.0055
Scenario 4 (V1G)	3.5110	0.4888	0.0000	3.9997
Scenario 5 (V1G-O)	3.5099	0.4881	0.0000	3.9980
Scenario 6 (V1G-F)	3.5065	0.4877	0.0000	3.9941
Scenario 7 (V2G)	3.7542	0.5229	0.0000	4.2771
Scenario 8 (V2G-O)	3.9312	0.5466	−4.4498	0.0280
Scenario 9 (V2G-F)	3.7586	0.5226	−13.3495	−8.3830
Tesla-Model Y (Unit: ¥/100 km)				
Scenario 1 (V0G)	3.3122	0.4610	0.0000	3.7732
Scenario 2 (V0G)	3.3114	0.4599	5.7581	3.7712
Scenario 3 (V0G)	3.3157	0.4605	0.0000	3.7761
Scenario 4 (V1G)	3.3112	0.4611	0.0000	3.7723
Scenario 5 (V1G-O)	3.3087	0.4602	0.0000	3.7690
Scenario 6 (V1G-F)	3.3066	0.4599	0.0000	3.7665
Scenario 7 (V2G)	3.7709	0.5254	0.0000	4.2963
Scenario 8 (V2G-O)	3.7889	0.5271	−5.6988	−1.3828
Scenario 9 (V2G-F)	3.5563	0.4945	−12.4338	−8.3830

Notes: Here, "Fuel" refers to the fuel cost, "Carbon" to the social cost of carbon emissions, "Capacity" to the generation capacity investment cost, and "Social Cost" is the sum of these three costs.

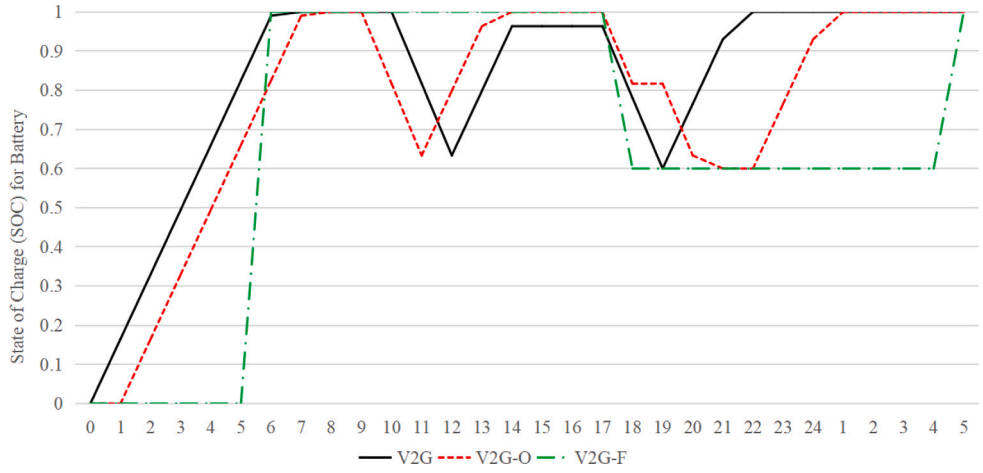

Fig. A.9. V2G charging and discharging scenario simulations (Tesla Model Y).

i and j are the hours of the day. $S_k^{i,\text{old}}$ is the incremental capacity investment cost attributed to charging during hour i, computed using Eq. (4). $S_k^{i,\text{old}} / \sum_{j=1}^{24} S_k^{j,\text{old}}$ indicates the weight (or relative share) of the hour i of the total incremental capacity requirement. Multiplying this weight by the daily maximum incremental capacity cost, $\max_{j=1,\ldots,24} S_k^{j,\text{old}}$, yields $S_k^{i,\text{new}}$, the reallocated capacity investment cost corresponding to hour i.

Additionally, fuel and carbon emissions costs for each hour are computed using Eqs. (2) and (3), respectively. By aggregating these three cost components, we obtain the social costs for charging in hour i, denoted as S^i. Averaging S^i across 365 days and dividing it by the corresponding total charging load yields an hourly efficient time-of-use tariff P^i, as illustrated in Fig. 7.

A.5. Table appendix

Table A.2 presents information on the thermal efficiency and emission factors of five categories of fossil fuel power plants: small, medium-sized, and large coal-fired power plants, as well as single- and double-shaft CCGTs in Guangdong.

Tables A.3 and A.4 present the specific values reflecting the impact of transportation electrification on the social costs in Guangdong and Gansu provinces, respectively, across the nine proposed scenarios (recall Section 4.2).

A.6. Figure appendix

Fig. A.9 shows the variation of a Tesla Model Y's battery State of Charge (SOC) over time under V2G (Scenario 7), Optimal V2G

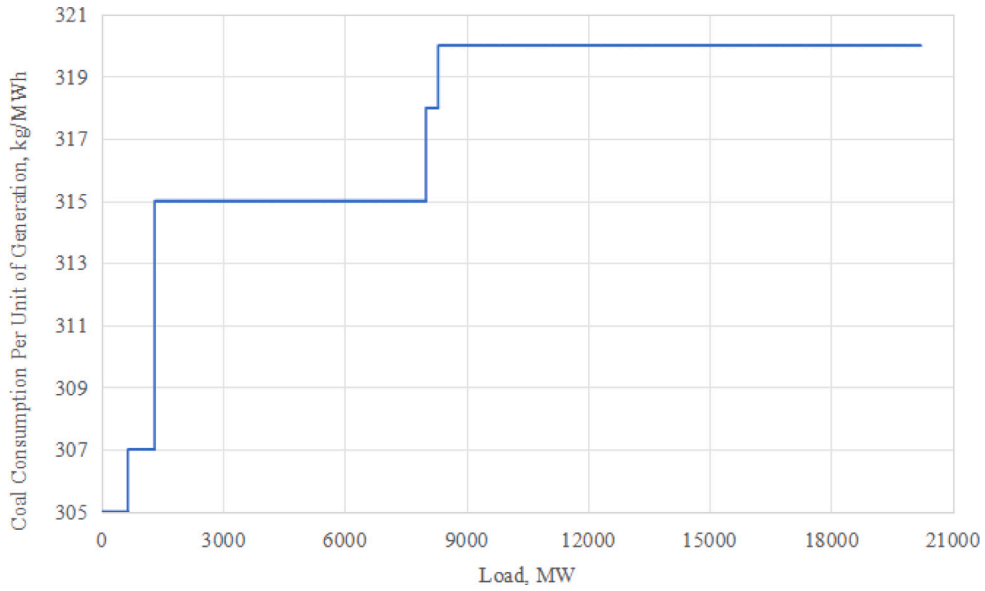

Fig. A.10. Merit-order curve in Gansu in 2022.

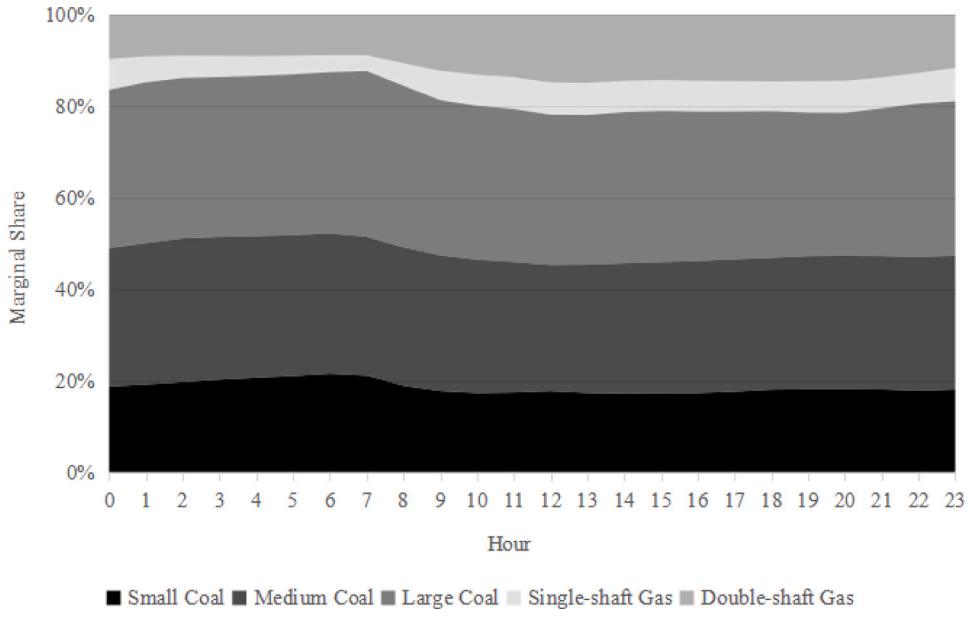

Fig. A.11. Composition of marginal power plants in Guangdong, October 2021–September 2022.

(Scenario 8), and V2G using fast charging technology (Scenario 9) in Guangdong (recall Section 4.2). Among them, V2G is determined by the peak–valley time periods officially designated by Guangdong province, while V2G-O and V2G-F are formulated based on the actual market-traded load in Guangdong province.

Fig. A.10 shows the merit-order curve for Gansu province, which is constructed from the power generation costs in Gansu. Most of the marginal fluctuations in the market-traded load are attributed to coal plants with per MWh generation costs of 315 kg of coal consumption, referring to the market-traded load of Gansu in 2022 (recall Fig. 3(b)).

Fig. A.11 depicts the composition of marginal power plants in Guangdong province, estimated based on actual power dispatch data. Approximately 82% of the marginal fluctuations in the market-traded load originate from coal plants, with gas turbines accounting for the remainder. Considering the market-traded load of Guangdong (recall Fig. 3(a)), coal plants served as marginal plants with a higher frequency during low-market-traded-load hours than during high-market-traded-load hours.

References

Abdelfattah, W., Abdelhamid, A.S., Hasanien, H.M., Rashad, B.A.-E., 2024. Smart vehicle-to-grid integration strategy for enhancing distribution system performance and electric vehicle profitability. Energy 302, 131807.

Al-obaidi, A.A., Farag, H.E.Z., 2024. Optimal design of V2G incentives and V2G-capable electric vehicles parking lots considering cost-benefit financial analysis and user participation. IEEE Trans. Sustain. Energy 15 (1), 454–465.

Archsmith, J., Kendall, A., Rapson, D., 2015. From cradle to junkyard: assessing the life cycle greenhouse gas benefits of electric vehicles. Res. Transp. Econ. 52, 72–90.

Bailey, M.R., Brown, D.P., Myers, E., Shaffer, B.C., Wolak, F.A., 2024. Electric vehicles and the energy transition: Unintended consequences of a common retail rate design. Technical report, National Bureau of Economic Research.

Bailey, M.R., Brown, D.P., Shaffer, B.C., Wolak, F.A., 2023. Show me the money! incentives and nudges to shift electric vehicle charge timing. Technical report, National Bureau of Economic Research.

Burlig, F., Bushnell, J., Rapson, D., Wolfram, C., 2021. Low energy: Estimating electric vehicle electricity use. In: AEA Papers and Proceedings, 111, American Economic Association 2014 Broadway, Suite 305, Nashville, TN 37203, pp. 430–435.
Callaway, D.S., Fowlie, M., McCormick, G., 2018. Location, location, location: The variable value of renewable energy and demand-side efficiency resources. J. Assoc. Environ. Resour. Econ. 5 (1), 39–75.
Chyong, C.K., Guo, B., Newbery, D., 2020. The impact of a Carbon Tax on the CO2 emissions reduction of wind. Energy J. 41 (1), 1–32.
Cullen, J., 2013. Measuring the environmental benefits of wind-generated electricity. Am. Econ. J.: Econ. Policy 5 (4), 107–133.
Davis, L.W., 2019. How much are electric vehicles driven? Appl. Econ. Lett. 26 (18), 1497–1502.
Geske, J., Schumann, D., 2018. Willing to participate in vehicle-to-grid (V2G)? Why not!. Energy Policy 120, 392–401.
Gillingham, K.T., van Benthem, A.A., Weber, S., Saafi, M.A., He, X., 2023. Has consumer acceptance of electric vehicles been increasing? evidence from microdata on every new vehicle sale in the united states. In: AEA Papers and Proceedings, vol. 113, American Economic Association 2014 Broadway, Suite 305, Nashville, TN 37203, pp. 329–335.
Gomes, I.S.F., Abdin, A.F., Puchinger, J., Perez, Y., 2024. Unlocking flexible electric vehicle charging via new rate design. Energy J. 45 (3), 231–272.
Greaker, M., Hagem, C., Proost, S., 2022. An economic model of vehicle-to-grid: Impacts on the electricity market and consumer cost of electric vehicles. Resour. Energy Econ. 69, 101310.
Green II, R.C., Wang, L., Alam, M., 2011. The impact of plug-in hybrid electric vehicles on distribution networks: A review and outlook. Renew. Sustain. Energy Rev. 15 (1), 544–553.
Guille, C., Gross, G., 2009. A conceptual framework for the vehicle-to-grid (V2G) implementation. Energy Policy 37 (11), 4379–4390.
Guo, B., Sun, A., Song, F., 2023. Time is money: The social benefits of time-of-use tariffs. SSRN Work. Pap. (4560864).
Holland, S.P., Mansur, E.T., Muller, N.Z., Yates, A.J., 2016. Are there environmental benefits from driving electric vehicles? The importance of local factors. Am. Econ. Rev. 106 (12), 3700–3729.
Holland, S.P., Mansur, E.T., Muller, N.Z., Yates, A.J., 2019. Distributional effects of air pollution from electric vehicle adoption. J. Assoc. Environ. Resour. Econ. 6 (S1), S65–S94.
IEA, 2023. World Energy Outlook 2023. International Energy Agency, Paris.
Lee, W., Woo, J., gun Kim, Y., Koo, Y., 2024. Vehicle-to-grid as a competitive alternative to energy storage in a renewable-dominant power system: An integrated approach considering both electric vehicle drivers' willingness and effectiveness. Energy 310, 133194.
Li, S., Tong, L., Xing, J., Zhou, Y., 2017. The market for electric vehicles: indirect network effects and policy design. J. Assoc. Environ. Resour. Econ. 4 (1), 89–133.
Ma, S.-C., Yi, B.-W., Fan, Y., 2022. Research on the valley-filling pricing for EV charging considering renewable power generation. Energy Econ. 106, 105781.
McCollum, D.L., Wilson, C., Bevione, M., Carrara, S., Edelenbosch, O.Y., Emmerling, J., Guivarch, C., Karkatsoulis, P., Keppo, I., Krey, V., et al., 2018. Interaction of consumer preferences and climate policies in the global transition to low-carbon vehicles. Nat. Energy 3 (8), 664–673.
Muehlegger, E.J., Rapson, D.S., 2023. Correcting estimates of electric vehicle emissions abatement: Implications for climate policy. J. Assoc. Environ. Resour. Econ. 10 (1), 263–282.
Nagel, N.O., Jåstad, E.O., Martinsen, T., 2024. The grid benefits of vehicle-to-grid in Norway and Denmark: An analysis of home- and public parking potentials. Energy 293, 130729.
NEA, 2020. Projected costs of generating electricity-2020 edition. Technical report, OECD Publishing, Paris.
Needell, Z.A., McNerney, J., Chang, M.T., Trancik, J.E., 2016. Potential for widespread electrification of personal vehicle travel in the United States. Nat. Energy 1 (9), 1–7.
Nehiba, C., 2024. Electric vehicle usage, pollution damages, and the electricity price elasticity of driving. J. Environ. Econ. Manag. 124, 102915.
Newbery, D., 2021. National energy and climate plans for the island of Ireland: wind curtailment, interconnectors and storage. Energy Policy 158, 112513.
Newbery, D.M., 2023. High renewable electricity penetration: Marginal curtailment and market failure under 'subsidy-free' entry. Energy Econ. 126, 107011.
Newbery, D., 2025. Implications of renewable electricity curtailment for delivered costs. Energy Econ. 145, 108472.
Newbery, D.M., Biggar, D.R., 2024. Marginal curtailment of wind and solar PV: Transmission constraints, pricing and access regimes for efficient investment. Energy Policy 191, 114206.
Novan, K., 2015. Valuing the wind: Renewable energy policies and air pollution avoided. Am. Econ. J.: Econ. Policy 7 (3), 291–326.
Novan, K., Wang, Y., 2024. Estimates of the marginal curtailment rates for solar and wind generation. J. Environ. Econ. Manag. 124, 102930.
Peterson, S.B., Michalek, J.J., 2013. Cost-effectiveness of plug-in hybrid electric vehicle battery capacity and charging infrastructure investment for reducing US gasoline consumption. Energy Policy 52, 429–438.
Powell, S., Cezar, G.V., Min, L., Azevedo, I.M., Rajagopal, R., 2022. Charging infrastructure access and operation to reduce the grid impacts of deep electric vehicle adoption. Nat. Energy 7 (10), 932–945.
Ricke, K., Drouet, L., Caldeira, K., Tavoni, M., 2018. Country-level social cost of carbon. Nat. Clim. Chang. 8 (10), 895–900.
Sagaria, S., van der Kam, M., Boström, T., 2025. Vehicle-to-grid impact on battery degradation and estimation of V2g economic compensation. Appl. Energy 377, 124546.
Shen, W., Han, W., Wallington, T.J., Winkler, S.L., 2019. China electricity generation greenhouse gas emission intensity in 2030: implications for electric vehicles. Environ. Sci. Technol. 53 (10), 6063–6072.
Sioshansi, R., Denholm, P., 2010. The value of plug-in hybrid electric vehicles as grid resources. Energy J. 31 (3), 1–24.
Sovacool, B.K., Axsen, J., Kempton, W., 2017. The future promise of vehicle-to-grid (V2G) integration: A sociotechnical review and research agenda. Annu. Rev. Environ. Resour. 42, 377–406.
Springel, K., 2021. Network externality and subsidy structure in two-sided markets: Evidence from electric vehicle incentives. Am. Econ. J.: Econ. Policy 13 (4), 393–432.
Suel, E., Xin, Y., Wiedemann, N., Nespoli, L., Medici, V., Danalet, A., Raubal, M., 2024. Vehicle-to-grid and car sharing: Willingness for flexibility in reservation times in Switzerland. Transp. Res. Part D: Transp. Environ. 126, 104014.
Taalbi, J., Nielsen, H., 2021. The role of energy infrastructure in shaping early adoption of electric and gasoline cars. Nat. Energy 6 (10), 970–976.
Thompson, A.W., Perez, Y., 2020. Vehicle-to-everything (V2X) energy services, value streams, and regulatory policy implications. Energy Policy 137, 111136.
Tian, P., Mao, B., Tong, R., Zhang, H., Zhou, q., 2023. Analysis of carbon emission level and intensity of China's transportation industry and different transportation modes. Adv. Clim. Chang. Res. 19 (3), 347.
van Heuveln, K., Ghotge, R., Annema, J.A., van Bergen, E., van Wee, B., Pesch, U., 2021. Factors influencing consumer acceptance of vehicle-to-grid by electric vehicle drivers in the netherlands. Travel. Behav. Soc. 24, 34–45.
Waraich, R.A., Galus, M.D., Dobler, C., Balmer, M., Andersson, G., Axhausen, K.W., 2013. Plug-in hybrid electric vehicles and smart grids: Investigations based on a microsimulation. Transp. Res. Part C: Emerg. Technol. 28, 74–86.
Wei, W., Ramakrishnan, S., Needell, Z.A., Trancik, J.E., 2021. Personal vehicle electrification and charging solutions for high-energy days. Nat. Energy 6 (1), 105–114.
Wikner, E., Thiringer, T., 2018. Extending battery lifetime by avoiding high SOC. Appl. Sci. 8 (10), 1825.
Wu, W., Lin, B., 2021. Benefits of electric vehicles integrating into power grid. Energy 224, 120108.
Wu, C.-H., Tzeng, G.-H., Lin, R.-H., 2009. A novel hybrid genetic algorithm for kernel function and parameter optimization in Support Vector Regression. Expert Syst. Appl. 36 (3, Part 1), 4725–4735.
Xing, J., Leard, B., Li, S., 2021. What does an electric vehicle replace? J. Environ. Econ. Manag. 107, 102432.
Yang, S.Y., Woo, J., Lee, W., 2024. Assessing optimized time-of-use pricing for electric vehicle charging in deep vehicle-grid integration system. Energy Econ. 138, 107852.
Yun, S., Woo, J., Kwak, K., 2025. Unlocking peak shaving: How EV driver heterogeneity shapes V2G potential. Energy 329, 136773.
Zhang, C., Kitamura, H., Goto, M., 2024. Feasibility of vehicle-to-grid (V2G) implementation in Japan: A regional analysis of the electricity supply and demand adjustment market. Energy 311, 133317.
Zivin, J.S.G., Kotchen, M.J., Mansur, E.T., 2014. Spatial and temporal heterogeneity of marginal emissions: Implications for electric cars and other electricity-shifting policies. J. Econ. Behav. Organ. 107, 248–268.